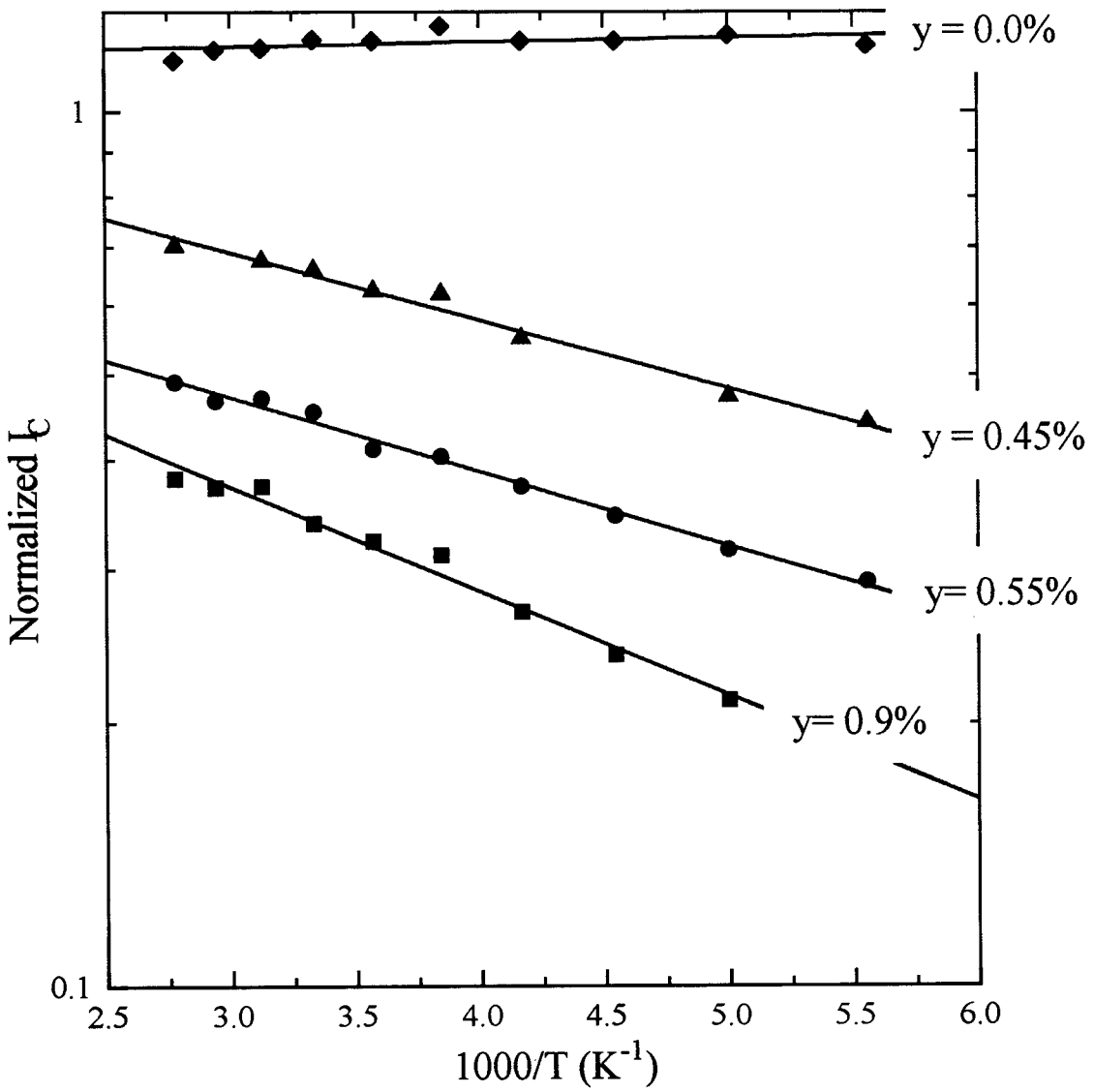

Figure 6.4: ($I_{C,\ SiGeC}/I_{C,\ SiGe}$) vs *1/T*.

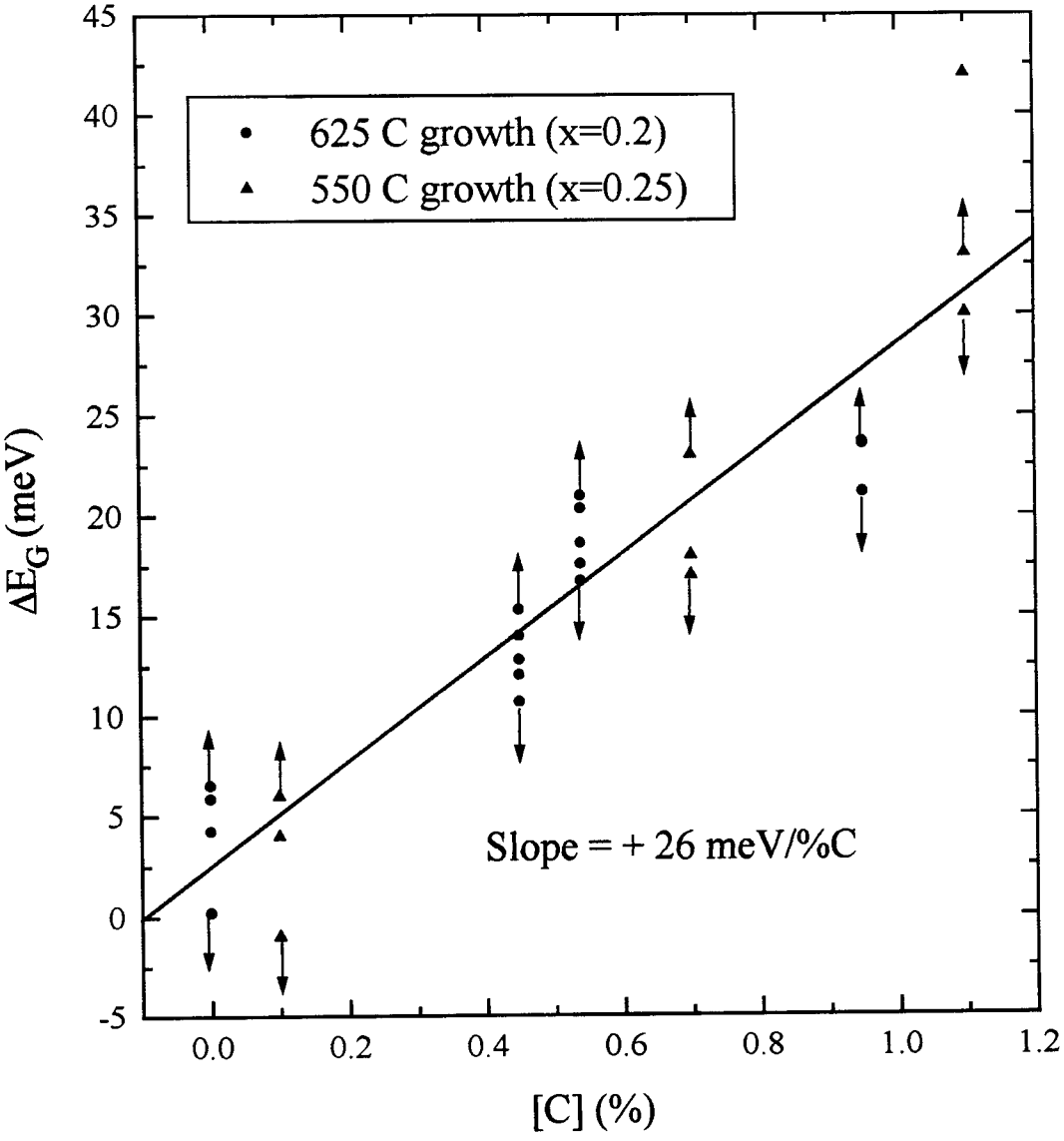

Figure 6.5: Extracted ΔE_G vs carbon fraction.
The vertical arrows represent the upper and lower limits of the error bars on the data points.

uniform throughout the material and hence the photoluminescence is not due to local centers.

6.4 Bandgap vs Strain for SiGeC and SiGe

Both electrical and photoluminescence data have shown that adding carbon to compressively strained SiGe on Si (100) increases the bandgap. This might be expected because incorporating carbon in SiGe relieves some of the strain which provides roughly 50% of the bandgap offset in SiGe, as shown in Figure 2.3. Strain relief in SiGe, either by carbon incorporation or dislocation formation, will move the strained SiGe bandgap towards that of the unstrained SiGe bandgap. In addition to the effects of strain relaxation on the bandgap of SiGe, the effect of the carbon atom on the bandgap needs to be considered. For example, the bandgap of the diamond is 5.3 eV which is quite a bit higher than the 1.1 eV bandgap of Si. Hence a combination of not only strain relaxation but also the carbon atom effect on the bandgap would be expected to determine the effect of carbon on the bandgap of SiGe.

Hence, to evaluate whether SiGeC is technologically more desirable than SiGe, one needs to evaluate the strain (critical thickness) vs. bandgap tradeoff of carbon in SiGe. For example, what are the technological advantages of SiGeC alloys over SiGe alloys if the bandoffset is lost by increasing carbon fraction? The key point to consider is that by adding carbon, strain is relieved, so that for carbon to be advantageous, it must relax the strain in the layer faster than it increases its bandgap.

Figure 6.6 shows the tradeoffs between bandgap and strain for both SiGe and SiGeC using photoluminescence as measured by St. Amour [20]. The photoluminescence

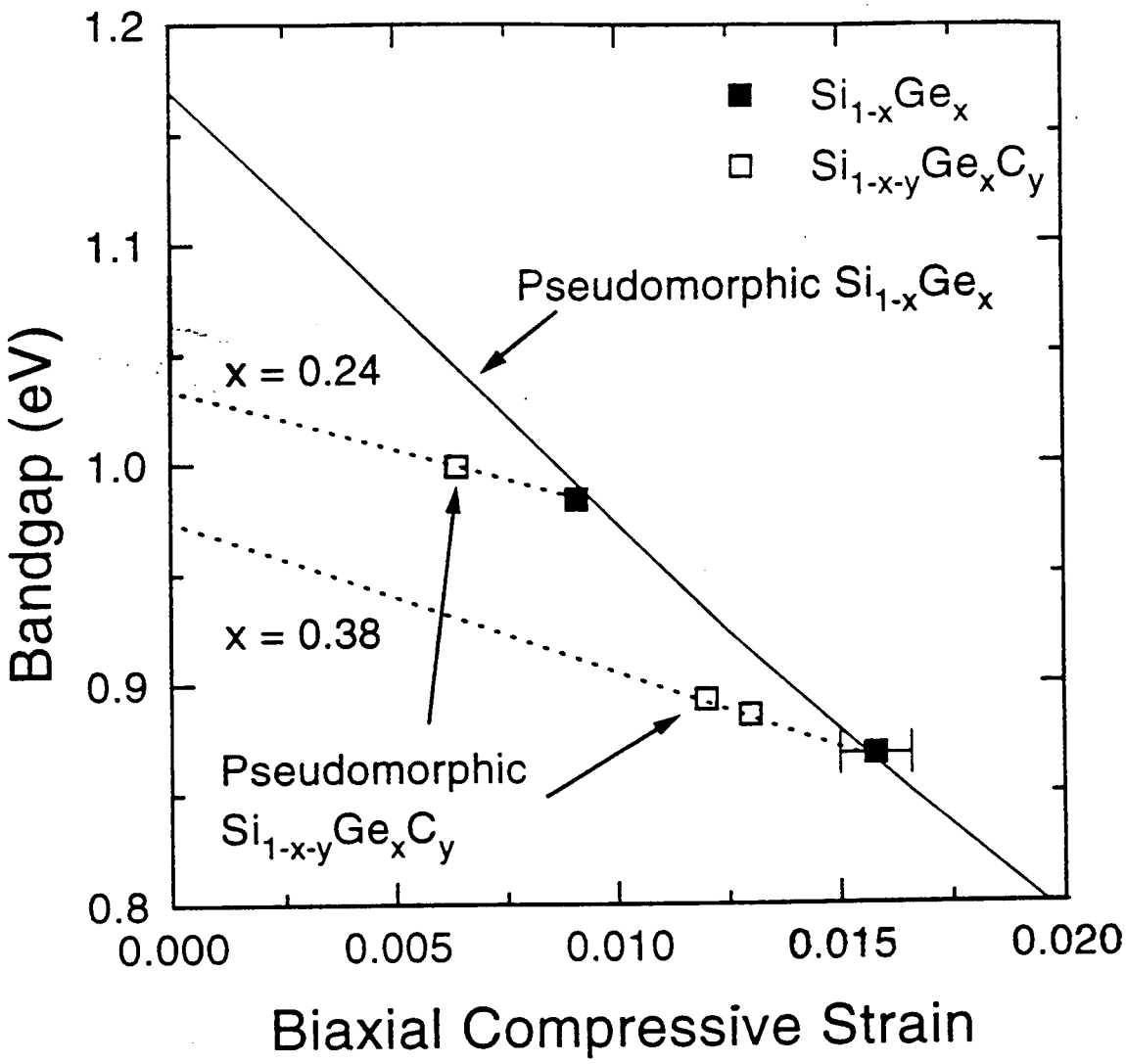

Figure 6.6: Figure showing the tradeoff between bandgap and strain for SiGe and SiGeC alloys.

measurements of +21 meV/%C are essentially identical to the HBT electrical results within the experimental error of both techniques. The solid line in Figure 6.6 plots the bandgap of SiGe vs. strain from pure silicon (0 strain) to roughly $Si_{0.5}Ge_{0.5}$ at 0.02 strain. The dotted lines show the bandgap of SiGeC vs. strain as carbon is added to a certain SiGe alloy. For example, as carbon is added to $Si_{0.62}Ge_{0.38}$, the bandgap is increased while the strain is reduced. Since the SiGeC data points fall to the left of the SiGe curve, this data shows that for a fixed strain (or identically, a fixed critical thickness, assuming similar mechanical properties of SiGe and SiGeC), a SiGeC sample has a lower bandgap than a pure SiGe sample. Consequently, SiGeC gives a larger bandgap offset than a SiGe sample at fixed strain. Alternatively, for a fixed bandgap, a SiGeC sample has a lower strain or equivalently a higher critical thickness than the SiGe sample. In other words, since the SiGeC data lies to the left of the SiGe bandgap vs. strain solid line, the ternary alloy SiGeC may promise to deliver material parameters which are simply impossible to achieve in the strained binary SiGe system. On the other hand, had the SiGeC bandgap data fallen to the right of the SiGe bandgap vs. strain curve, one could have concluded that SiGeC would not provide technological advantages over SiGe because at a fixed strain, a certain SiGe alloy would always have a lower bandgap than that possible with SiGeC alloys.

Using a change in bandgap of 26 meV/%C, the collector saturation currents of transistors with 0.5% and 0.9% C levels would decrease by factors of 1.7 and 2.5, assuming that the bandgap is the only parameter in Equation 2.2 which changes with carbon incorporation. This gives relatively good agreement with the experimentally measured changes in collector saturation current of 1.25 and 2, indicating that changes in collector saturation current between SiGe and SiGeC are due to, within experimental

error, changes in the base bandgap caused by carbon incorporation, and not due to changes in N_C, N_V, and D_n.

6.5 Base Currents in $Si_{1-x-y}Ge_xC_y$ HBTs

While changes in SiGeC HBT collector saturation current may be explained by changes in SiGeC bandgap, the increased base current with increasing carbon fraction is more difficult to explain, primarily because of non-ideal device base current. As shown in Figure 6.2, I_B increases a factor of ~10 in the $Si_{0.791}Ge_{0.2}C_{0.009}$ device compared with that of the $Si_{0.8}Ge_{0.2}$ control device. This increasing base current at high V_{BE} may be due to recombination in the neutral base caused by carbon induced traps. However, modeling base currents in regions without an ideal slope (60 mV/decade) is a difficult proposition, especially since a large portion of the nonideality comes from traps at the emitter-base interface due to oxygen incorporation. Ideally, new wafers should be grown with DCS emitters which then are processed using a structure which results in ideal base currents.

In order to verify that the base current increase did indeed come from the neutral base and not due, for example, emitter-base depletion region recombination [36-39], wafers were grown in which the doped SiGeC layers were sandwiched inside doped SiGe layers, as shown in Figure 6.7. Undoped SiGe spacers surround the doped SiGe/SiGeC/SiGe base. Thus, the doped 50 Å SiGe layers act as doped spacers surrounding the doped SiGeC within the base. These 50 Å doped SiGe spacer layers were designed to keep both the emitter-base and base-collector depletion regions from touching the doped SiGeC in the middle of the base. Hence these sandwich bases should isolate the

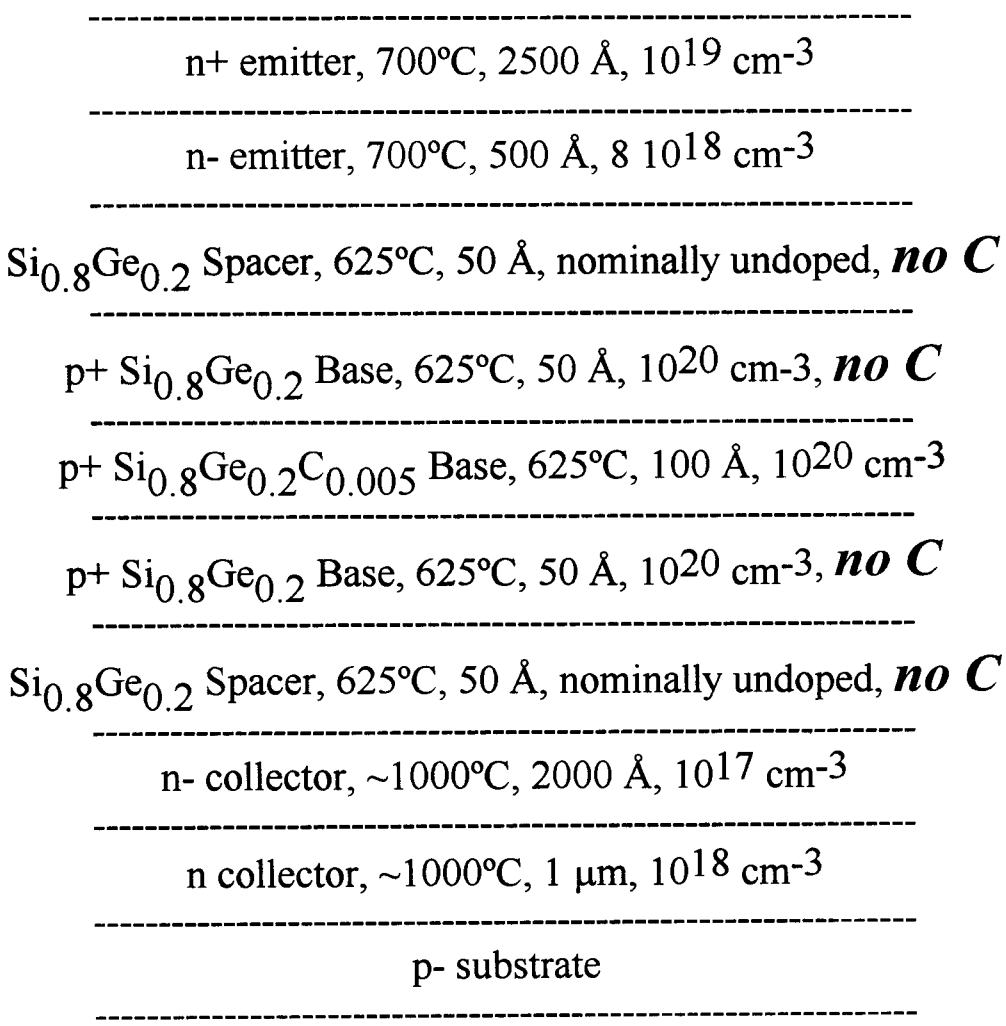

Figure 6.7: SiGeC sandwich base structure.

effects of depletion region recombination from the effects of neutral base recombination. Note that these devices contrast with the previously discussed SiGeC HBTs which had carbon in both the undoped base spacers as well as the doped base.

Figure 6.1 shows common-emitter and common-base characteristics of a 50 Å doped SiGe base (no carbon) to prove that 50 Å of 10^{20} cm^{-3} boron-doped SiGe is sufficient to prevent the depletion regions from touching the carbon layers. In other words, a 50 Å 10^{20} cm^{-3} doped base does not suffer from punchthrough of the emitter-base and base-collector space charge regions under normal operating conditions.

Two wafers were grown, one with 0.5% C and the other with 0.9% C sandwiched inside the base. Thus the sandwich bases have total SiGe and SiGeC alloy thicknesses of 300 Å, 200 Å of which is doped 10^{20} cm^{-3} boron. As shown in Figure 6.7, the first 100 Å of the base is SiGe, the second 100 Å is SiGeC, the third 100 Å is SiGe. Common-base characteristics of the sandwich bases are shown in Figure 6.8 along with the characteristics from a SiGe 200 Å doped base (no carbon) and a $Si_{0.795}Ge_{0.2}C_{0.005}$ 200 Å doped base. The I_B characteristics have a general trend of shifting from n=2 at low current levels (characteristic of space charge recombination) to near n=1 at high current levels, (characteristic of neutral base recombination).

At V_{EB} = -0.6 V, the transistor with the lowest base current is, as expected from Figure 6.2, the no C sample. The $Si_{0.795}Ge_{0.2}C_{0.005}$ sandwich base sample's base current is larger than the no carbon sample by roughly a factor of ~1.4, indicating that depletion region recombination is not the source of the increase in base current. The device with $Si_{0.795}Ge_{0.2}C_{0.005}$ throughout the entire base has a larger base current than the 0.5% C sandwich base since there is more integrated carbon in the base. The $Si_{0.791}Ge_{0.2}C_{0.009}$ sandwich device's base currents are the highest of all. Had the sandwich devices' base currents been identical to that of the no-carbon transistor's base

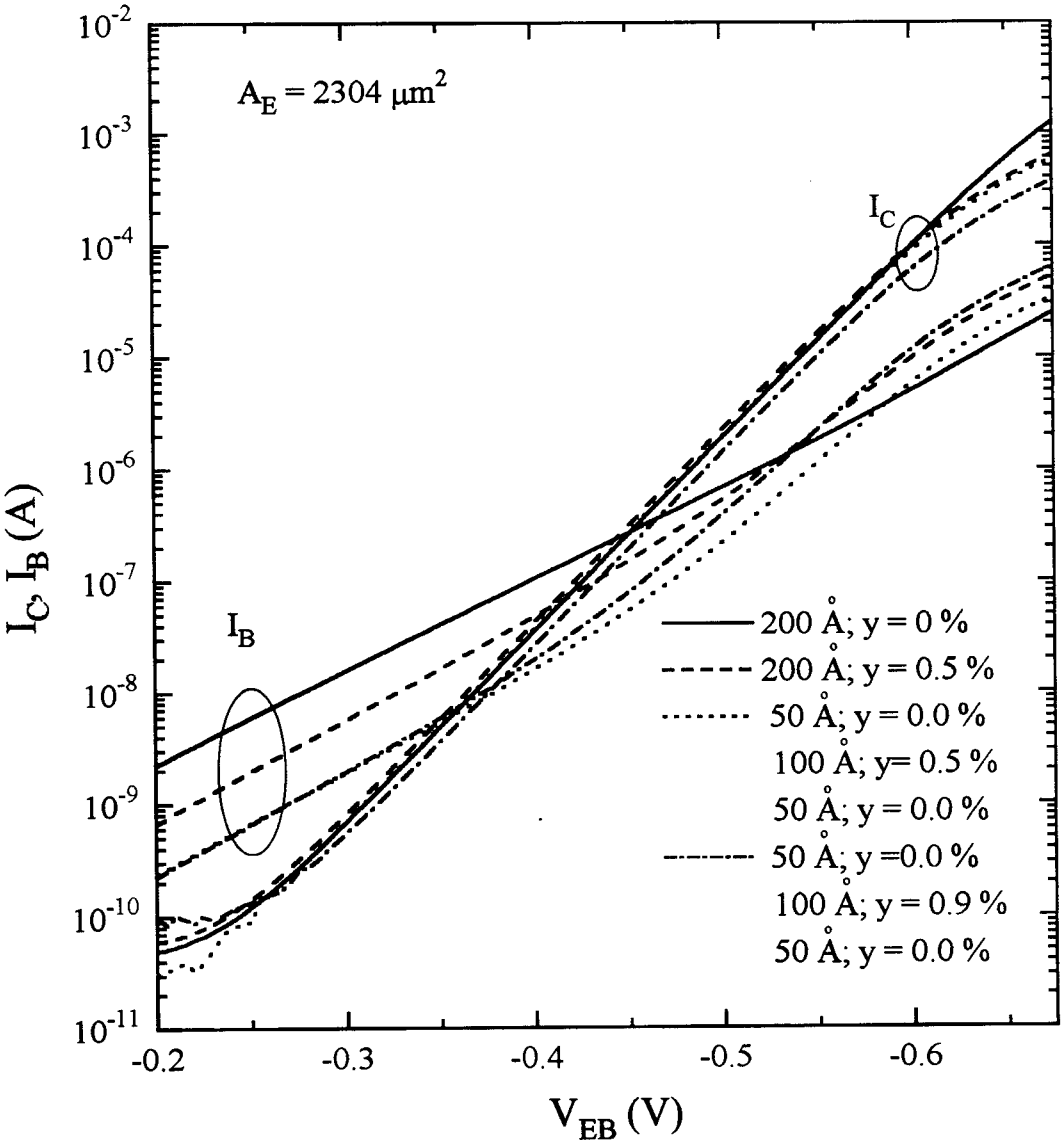

Figure 6.8: Common Base Characteristics of $Si_{1-x-y}Ge_xC_y$ Uniform Base and Sandwich Base HBTs. The legend indicates the doped base structure and does not include the 50 A undoped SiGe(C) spacers in all structures.

currents, one could conclude that the increase in base currents is due to carbon in the depletion region. However, the fact that the base currents increase when C is inside the neutral base suggests that C causes increases in neutral base recombination by causing a reduction in minority carrier lifetime with increasing carbon fractions. The base current characteristics at low V_{BE} are not reproducible from device to device and from wafer to wafer.

From the increase in base current with increasing carbon fraction, one may extract a minority carrier lifetime as shown in Figure 6.9. Without ideal base currents and more data points, however, this data is of questionable merit..

6.6 Summary

$Si_{1-x-y}Ge_xC_y$ HBTs have been demonstrated with carbon concentrations less than 0.9% C. The temperature dependence of their saturation currents were used to measure a change in bandgap of + 26 meV/%C between $Si_{1-x}Ge_x$ and $Si_{1-x-y}Ge_xC_y$. Using these results and knowledge of the reduction in strain caused by carbon incorporation, $Si_{1-x-y}Ge_xC_y$ alloys have been shown to provide possible technological advantages over $Si_{1-x}Ge_x$ alloys. However, the base current in SiGeC HBTs increases with carbon fraction. The decrease in current gain caused by this base current increase may be due to an increase in neutral base recombination caused by carbon incorporation.

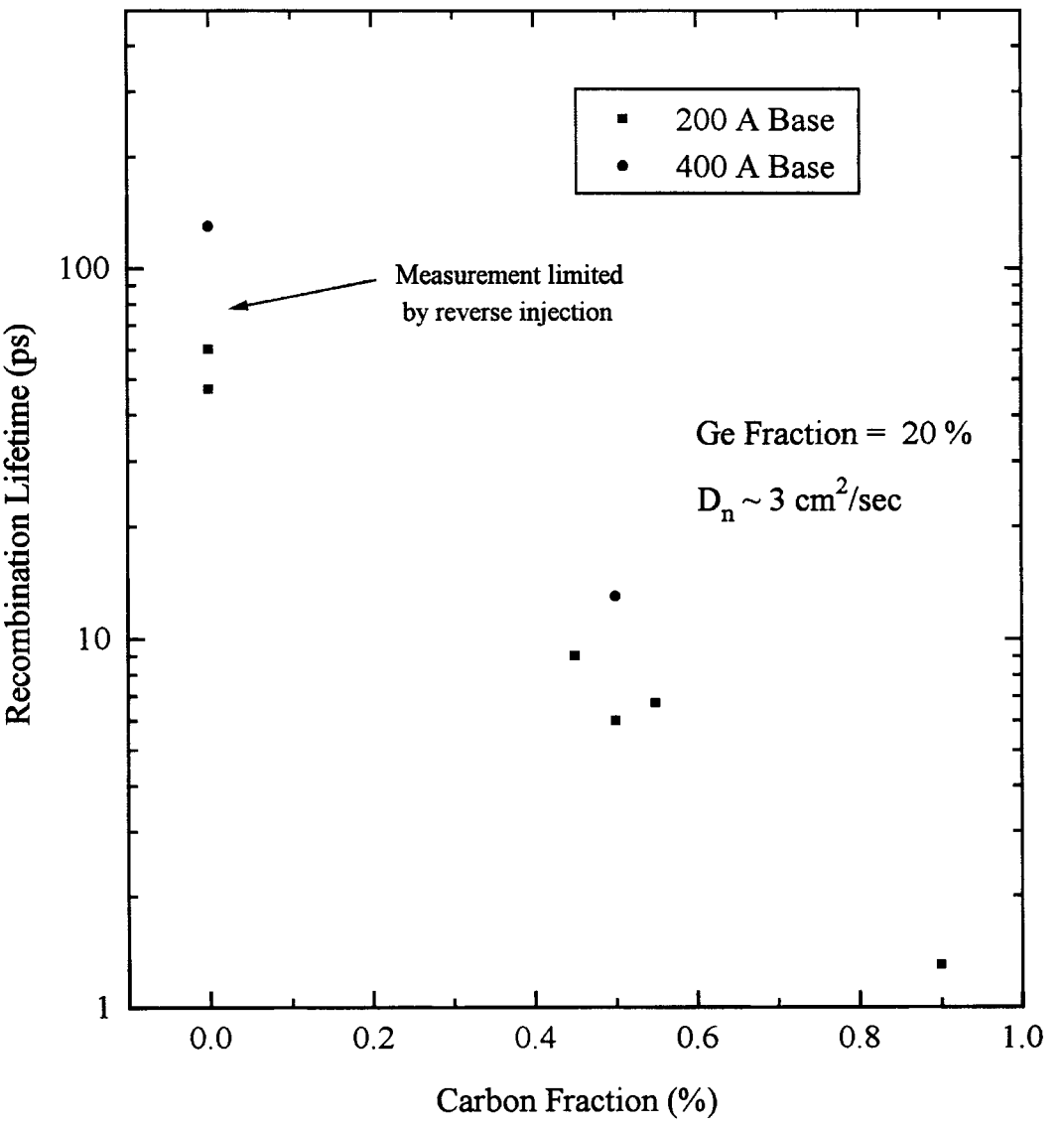

Figure 6.9: Extraction of minority carrier lifetime as a function of carbon from current gain.

Chapter 7

The Effects of Carbon on Boron Diffusion in SiGe HBTs

7.1 Introduction

In the previous chapter we explored the effect of carbon on the electrical properties of SiGeC alloys. In this chapter, we demonstrate that carbon also has very beneficial effects on processing properties of SiGeC, specifically with respect to boron diffusion. To first understand boron diffusion effects in HBTs, we will first review why ion implantation, which causes transient enhanced diffusion (TED) of boron, is used in HBT processing. Ion implantation is typically used to form highly doped regions for ohmic contacts to emitter or extrinsic base regions, especially when trying to avoid mesa processing of the emitter. After a historical perspective of TED effects in SiGe HBTs, we will examine the effect of carbon on boron diffusion, which was studied by using HBT electrical changes as described in Section 4.4.

7.2 HBT process using emitter and extrinsic base ion implanted contacts

A simple university style, but nevertheless "manufacturable", ideal-base current SiGe HBT process was among the first SiGe HBTs demonstrated [96]. It used implanted emitter contacts and implanted extrinsic base contacts, as shown in Figure 7.1 to contact the emitter and base, respectively. In fact, the devices from Figure 2.6 were fabricated using it [15] and this device structure was demonstrated before that of the far simpler double mesa process used throughout this thesis [24].

This ideal base current process, as shown in Figure 7.1, starts with the growth of the lightly doped n-type collector, the p-type SiGe base, and then a lightly doped n-type silicon emitter. This is in contrast to the double mesa structure which uses an n+ Si layer to contact the lightly doped emitter. As shown in Figure 7.1, contact is made to the lightly doped emitter using a masked shallow arsenic implant whose range is roughly 1000 Å. Without the n+ emitter implantation, a metal contact to the 10^{17} cm^{-3} n-type emitter would be schottky rather than ohmic. Contact to the buried p-type base is made using masked extrinsic BF_2 and B implantation into the lightly doped emitter. This implantation turns the lightly doped n-type emitter p-type. The implanted boron surrounds the implanted emitter contact on all four sides so that the emitter-base depletion region is only exposed at the mesa surface. If a heavily doped n-type emitter had been grown to eliminate the necessity of arsenic implantation, parasitic tunneling currents from the side n+/p+ (implanted) junctions would lead to high non-ideal base currents [36-39], as will be shown shortly. Contact to the collector is made by masking the extrinsic base implants as well as the intrinsic device and plasma etching down to the subcollector, as shown in Figure 7.1. Metallization is then defined for the emitter, base, and collector. The critical

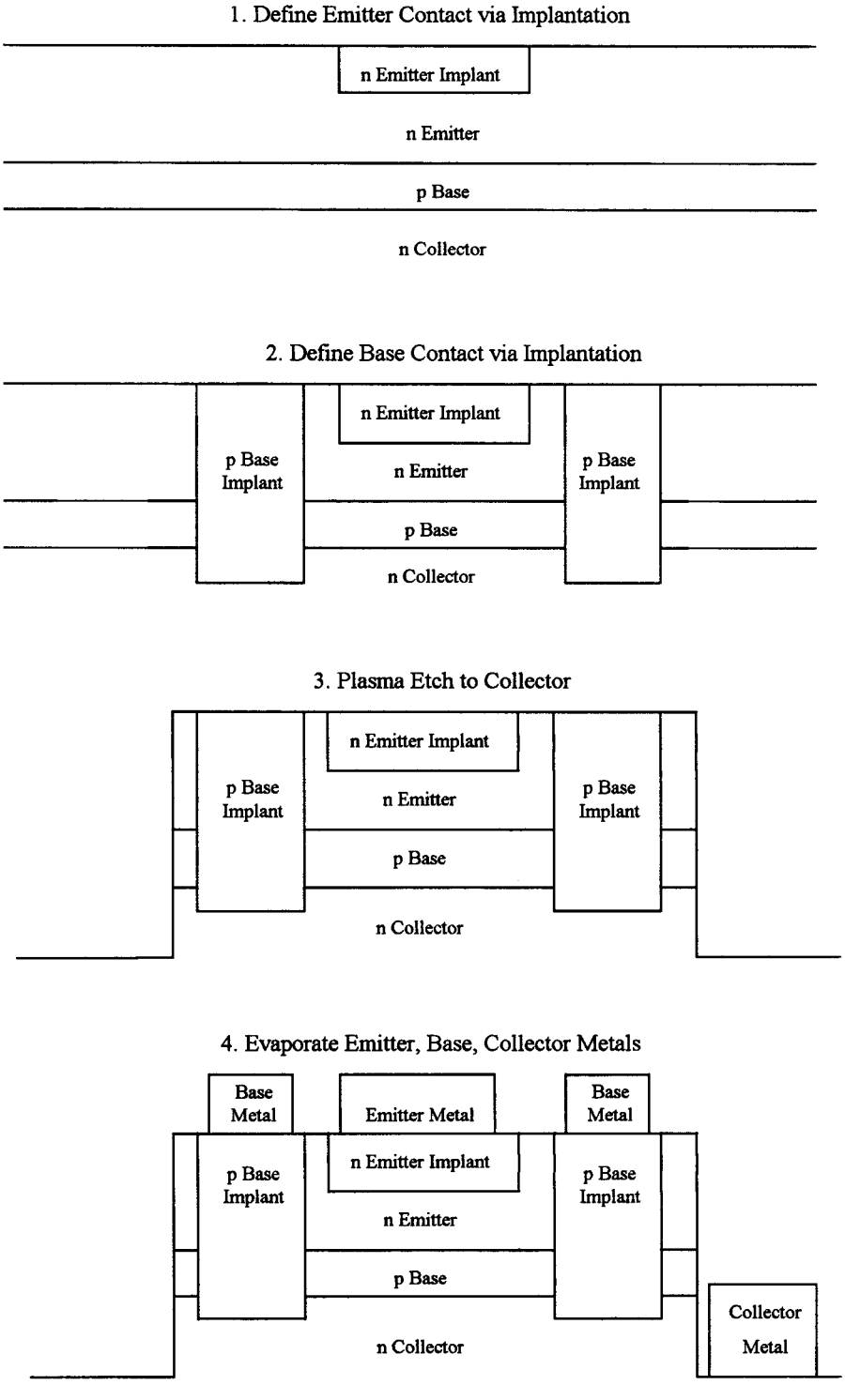

Figure 7.1: Ideal-base current process using implantation.

factor of this process is that it uses ion implantation, especially into the intrinsic device region for the emitter implant.

7.3 Transient Enhanced Diffusion

Transient enhanced diffusion is called "transient" because, at a fixed anneal temperature, most of the "enhanced" boron diffusion takes place within the first ~15 minutes of the thermal anneal [99, 100]. This results because of defects from the ion implantation process assisting the diffusion process. Annealing for longer than ~15 minutes at the same temperature will only cause the much slower standard diffusion to occur. More TED effects will occur, however, if the wafer is heated to a higher temperature. TED occurs in implanted boron dopant profiles as well as epitaxially grown dopant profiles buried below the implantation range [101, 102]. TED occurs in buried boron layers, such as SiGe bases, because excess interstitials generated by the implant in the emitter above the base diffuse down to the base causing enhanced diffusion during the activation anneal following the implant. Further research has shown that TED of buried boron layers caused by arsenic implantation is reduced in SiGe compared to Si [103]. Heavily doped, 100 Å wide boron spikes are so good at showing TED effects that boron doped superlattices are often used to measure TED of boron using SIMS profiling [104-107]. This thesis work has the advantage that it can monitor boron diffusion using both HBT electrical measurements as well as SIMS.

7.4 Introduction to Transient Enhanced Diffusion along with an Historical Perspective on $Si_{1-x}Ge_x$ HBTs

At this point it is important to give some historical background regarding SiGe HBTs, which, to the authors knowledge, has not been documented elsewhere. What was unknown at the time this ideal-base current transistor structure was developed at Stanford [96] was that excess interstitials created by both the arsenic and boron implants will diffuse from the implanted regions through the heavily doped intrinsic base during the dopant activation anneal. These excess interstitials greatly increase boron diffusion in the base, an effect which has come to be known as transient enhanced diffusion (TED). Epilayers undergoing the same thermal budget without implantation will only show the effects of normal, not enhanced, diffusion. Figure 7.2 compares the SIMS profiles of a 10^{20} cm^{-3} boron doped SiGe base following a 855°C thermal cycle for 15 minutes with the SIMS profile of a SiGe base following arsenic emitter implantation ($1.5x10^{15}$ cm^{-2} 30 keV, $3x10^{14}$ cm^{-2} 15 keV) and 755°C anneal for 15 minutes. Notice that following implantation and anneal, the boron in the SiGe base has undergone far more diffusion than that of the thermally annealed but not implanted base even though the thermal diffusion anneal temperature was 100°C higher. Such diffusion results in degraded HBT characteristics as described in Section 4.4.

Hence it should be impossible to fabricate, not-outdiffused 10^{20} cm^{-3} boron-doped SiGe base HBTs using this structure with implanted emitter and extrinsic base contacts. In other words, as shown in Figure 7.2, two 500 Å undoped SiGe spacer layers would be necessary to contain the boron diffusion, a thickness impossible to grow defect free with 20% germanium.

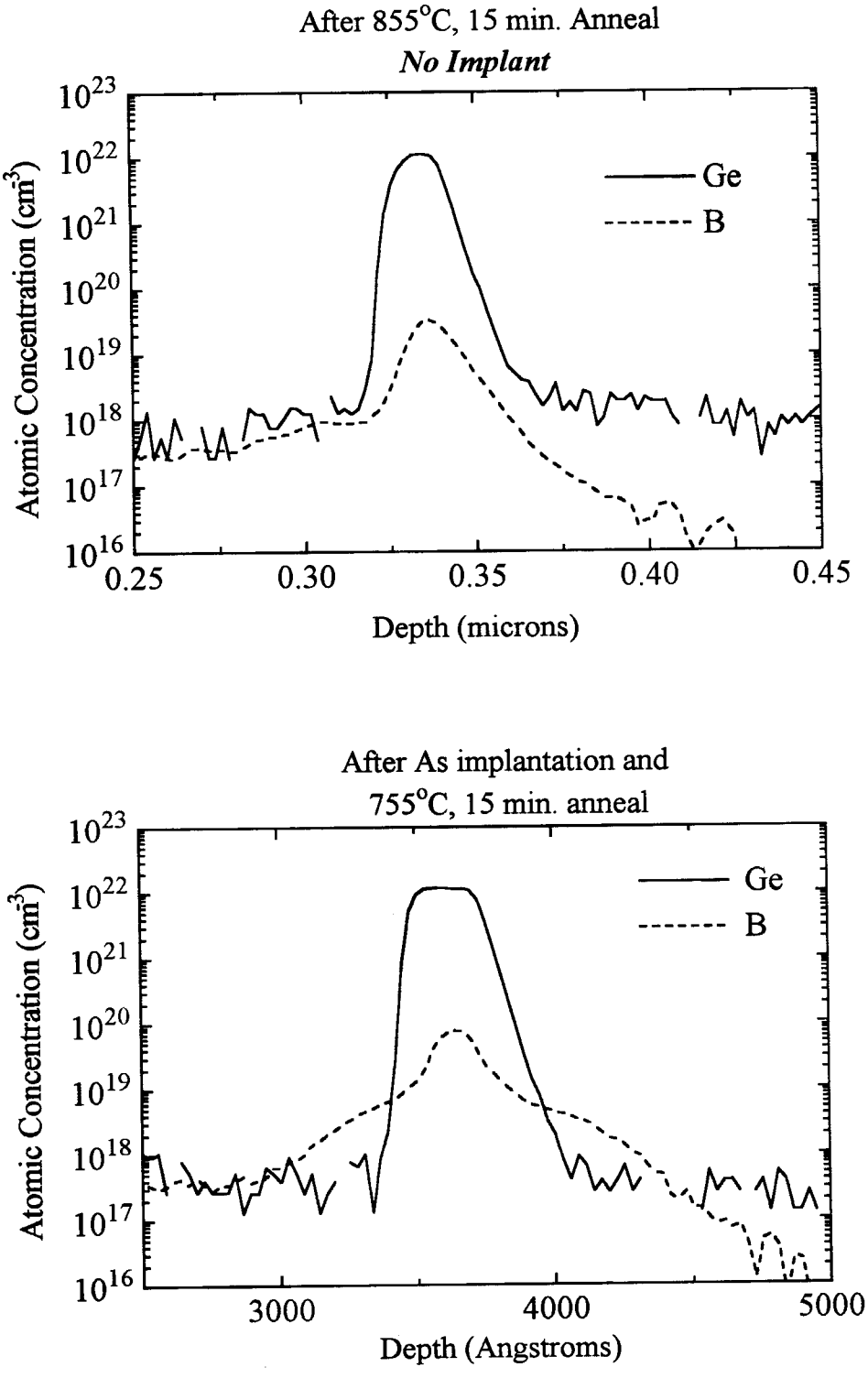

Figure 7.2: Comparison of thermal diffusion and TED conditions on boron profiles.

In the original Stanford experiments [96] using this process, however, the SiGe base unintentionally incorporated 10^{20} cm^{-3} oxygen atoms because the reactor had no load lock at that time [108]. It just so turns out, as was shown years later [109], that 10^{20} cm^{-3} oxygen concentrations in SiGe prevent TED from occurring in SiGe. Incidentally, the 10^{20} cm^{-3} oxygen concentration also degrades β by increasing I_B through neutral base recombination [96]. Thus, these first experiments [96], if not for the oxygen contamination, would not have produced the first CVD-grown HBTs without outdiffusion because of implantation related TED effects.

Furthermore, this author has also fabricated transistors from SiGe unintentionally doped 10^{20} cm^{-3} with oxygen using the double mesa process, but the transistors never "worked." Private communications with King has revealed that 10^{20} cm^{-3} oxygen doped SiGe bases will only "work" without any undoped SiGe spacers surrounding the heavily doped SiGe. (Presumably, the oxygen in the undoped SiGe spacers causes the p-n junctions to leak too badly for a transistor to function because the depletion layer then falls in the oxygen doped region. See section 7.8) King's transistors had no spacers because, at that time, problems associated with boron diffusion outside SiGe were not known and because, in any case, the unintentionally incorporated oxygen in the base eliminated these diffusion problems. Had King anticipated the need for undoped SiGe spacers to control boron diffusion, Stanford's "first" ideal base current, CVD grown, SiGe HBTs may not have "worked".

Subsequent SiGe HBT researchers at Princeton attached a load lock to their RTCVD reactor to eliminate the high oxygen levels in low-temperature-grown SiGe. These oxygen concentrations were associated with venting the growth chamber to atmosphere during the loading and unloading of samples [108]. Thus, researchers with low SiGe oxygen levels were not able to fabricate heavily-doped SiGe base HBTs without

boron outdiffusion using implantation [49] because oxygen was not in the SiGe to suppress TED. Prinz, however, was able to fabricate ideal-base current, transistors without boron outdiffusion using this process with boron levels of roughly $3x10^{18}$ cm^{-3} [97]. Since the collector was doped > 10^{17} cm^{-3} n-type, even though the boron underwent TED following arsenic implantation and anneal, the electrical effects were not as severe as if the base had been doped 10^{20} cm^{-3} with boron (Figure 7.2). These experiments led directly to the discovery of the importance of undoped SiGe spacer layers to compensate for any diffusion of boron [47], to the discovery of the importance of TED effects in SiGe HBTs [49, 50], and ultimately, to the development of SiGe HBT device structures which do not use implantation processes[8, 9, 110]. One of the lasting consequences of boron TED in SiGe HBTs is the absence of a manufacturable SiGe process which uses bases doped 10^{20} cm^{-3} with boron [111].

7.5 Effect of Extrinsic Base Implants on Boron TED in Si/SiGeC/Si HBTs

This work's first attempts at fabricating ideal-base current devices using the process from Figure 7.1 to analyze the increase in base currents associated with carbon incorporation used wafers intended for the double mesa process with a structure similar to that in Figure 7.1. Hence, emitter implantation was not needed due to the existence of the standard 10^{19} cm^{-3} phosphorus emitter contact layer. Thus, only extrinsic base implantation was used. Figure 7.3 shows Gummel plots of SiGe and SiGeC transistors fabricated following extrinsic base implantation ($5x10^{14}$ cm^{-2} 100 keV B+, $3x10^{14}$ cm^{-2} 60 keV B+, $3x10^{14}$ cm^{-2} 130 keV BF_2, $2x10^{14}$ cm^{-2} 45 keV BF_2, chosen to follow

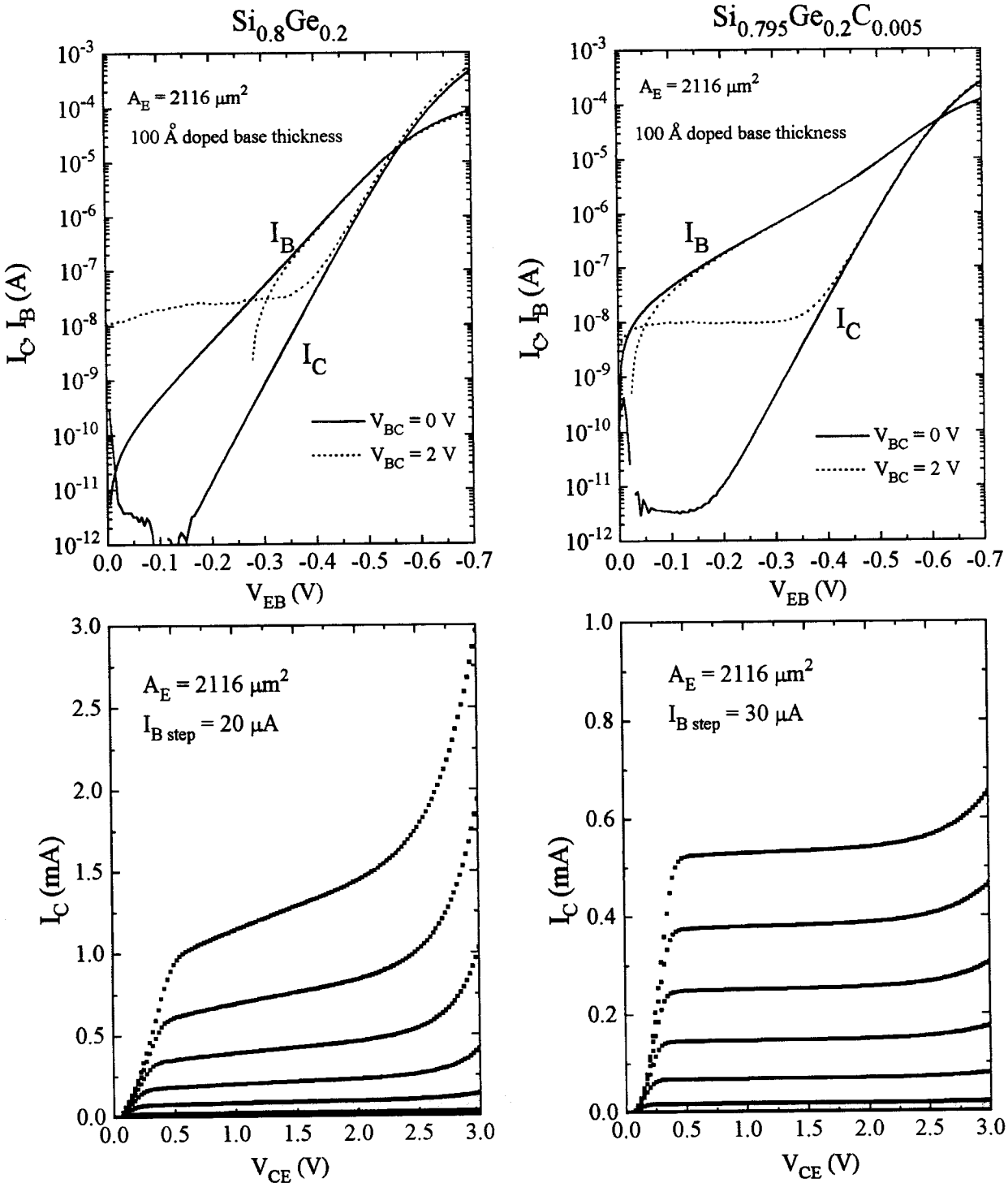

Figure 7.3: Transistors fabricated using extrinsic base implants and 655°C anneal.

[11]) and dopant activation at 655°C for 15 minutes in N_2. All of the anneals used for the rest of the chapter were also done in N_2. Figure 7.4 shows transistor characteristics of devices fabricated from pieces of the same wafers using the standard double mesa process which did not include any implantation and anneal. While the collector currents are nearly the same in both the mesa and ion implanted processes, instead of reducing the base current due to the mesa, the base currents are increased in the ion implanted structure. This is due to additional leakage current at the peripheral p+/n+ junction created at the p extrinsic base ion implant and n epitaxial grown emitter interface. To reduce this parasitic base current, a lightly doped, DCS emitter should be used together with a masked arsenic emitter contact.

Figure 7.3 plots the common-emitter characteristics for SiGe and SiGeC extrinsic base implanted structures while Figure 7.4 plots the common-emitter characteristics of the double mesa transistors. The Early voltages of both as-grown SiGe and SiGeC double mesa transistors are nearly identical, but following extrinsic base ion implantation and annealing, the Early voltage of the SiGe device has been degraded. However, the SiGeC implanted device's Early voltage is identical to that of the double mesa transistor. The degradation in Early voltage of the SiGe transistor is thought to be due to the outdiffusion of boron from the bases caused by interstitials generated during the extrinsic base implant which diffuse laterally during the activation anneal causing TED in the intrinsic base. The dopant which diffuses outside of the SiGe spacers results in lower transistor Early voltages. This TED mechanism of an intrinsic device degraded due to extrinsic base implants was demonstrated prior to these experiments [40, 112]. One must be certain that this outdiffusion is due to the peripheral boron implant and not caused, perhaps, by outdiffusion caused by excessively narrow spacer layers in pieces from the wafer edge, as

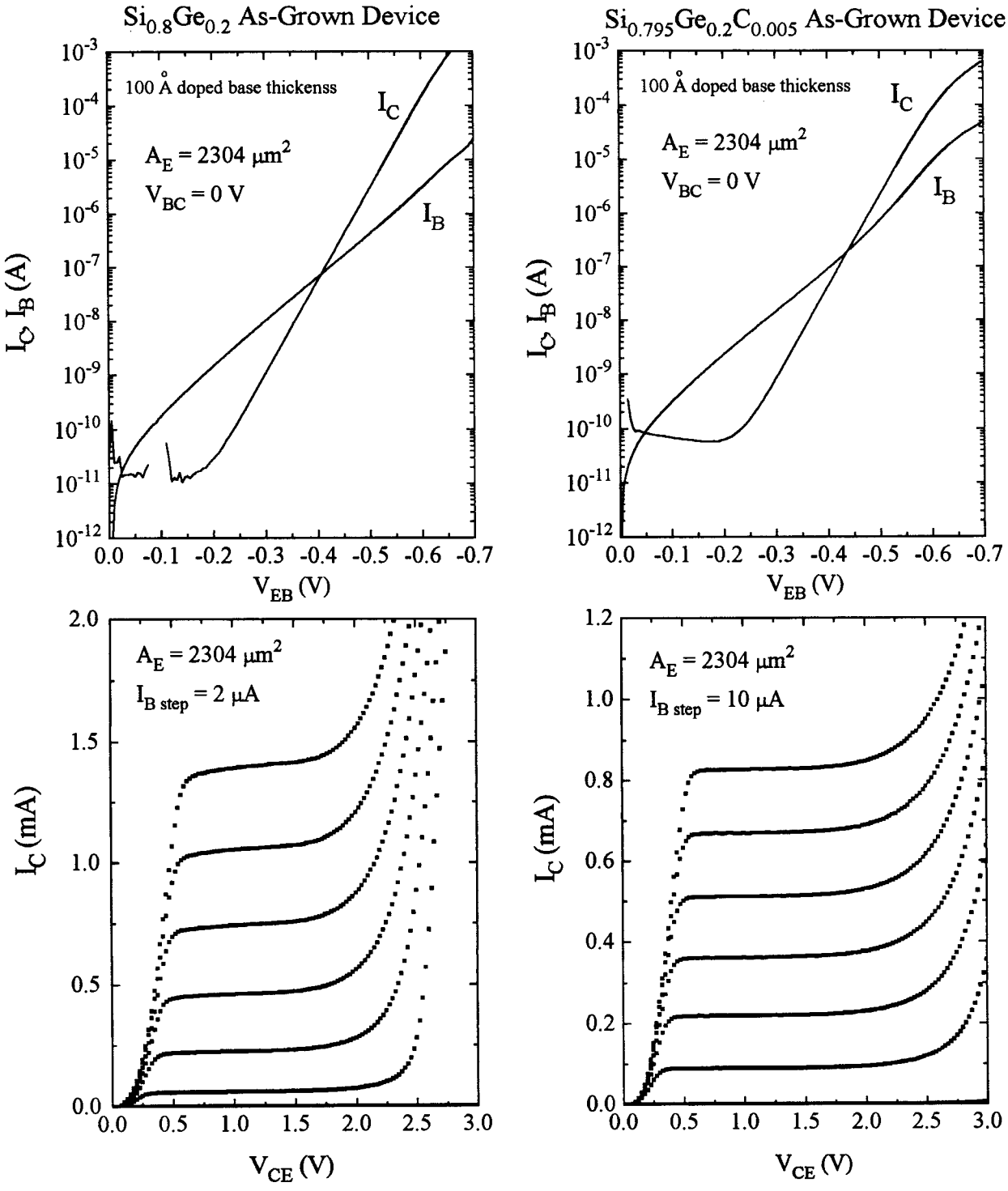

Figure 7.4: Double mesa, no implant, transistors fabricated from same wafers as used in Figure 7.3.

shown in Figure 4.17. The $Si_{1-x}Ge_x$ devices from Figures 7.3 and 7.4 came directly from the wafer center, however.

The question remains however, "Why is TED of boron suppressed in the SiGeC devices?" These results suggest that the carbon atom has some influence on TED of boron within the intrinsic base.

About the same time as these results were obtained, the author became aware of prior research concerning both implanted carbon [113] and epitaxially incorporated carbon [105, 114] in Si which showed that TED of boron was reduced in the presence of carbon. Poate et. al., as shown in Figure 7.5, have established, using 10^{19} cm^{-3} boron-doped superlattices grown in MBE material which incorporated a background concentration of $2x10^{19}$ cm^{-3} carbon, that carbon virtually eliminates TED of boron caused by a silicon implant and 790°C anneal [105, 114]. Their data illustrates the dramatic effect which substitutional carbon can have on boron diffusion properties. Following a silicon implant and 790°C anneal, the boron superlattice profiles with a background concentration of $2x10^{19}$ cm^{-3} carbon are identical to the as-grown boron superlattices whereas the no carbon sample's boron superlattices are spread out due to TED effects.

At that time, fortunately, Princeton had SiGeC base HBT wafers grown with 0.5% carbon fractions, doped 10^{20} cm^{-3} with boron along with SiGe (no carbon) control wafers. Hence, unknowingly, Princeton was in a perfect position to probe the effects of buried carbon layers on both boron thermal diffusion and TED using SiGe electrical devices. Knowing that normal thermal diffusion and TED of boron is a fundamental limit to heavily-doped SiGe HBT device integration and knowing that the electrical characteristics of SiGe HBTs can probe boron diffusion at a far more sensitive scale than SIMS, one should ask, "Can carbon be used to address the boron outdiffusion problems of SiGe HBTs?"

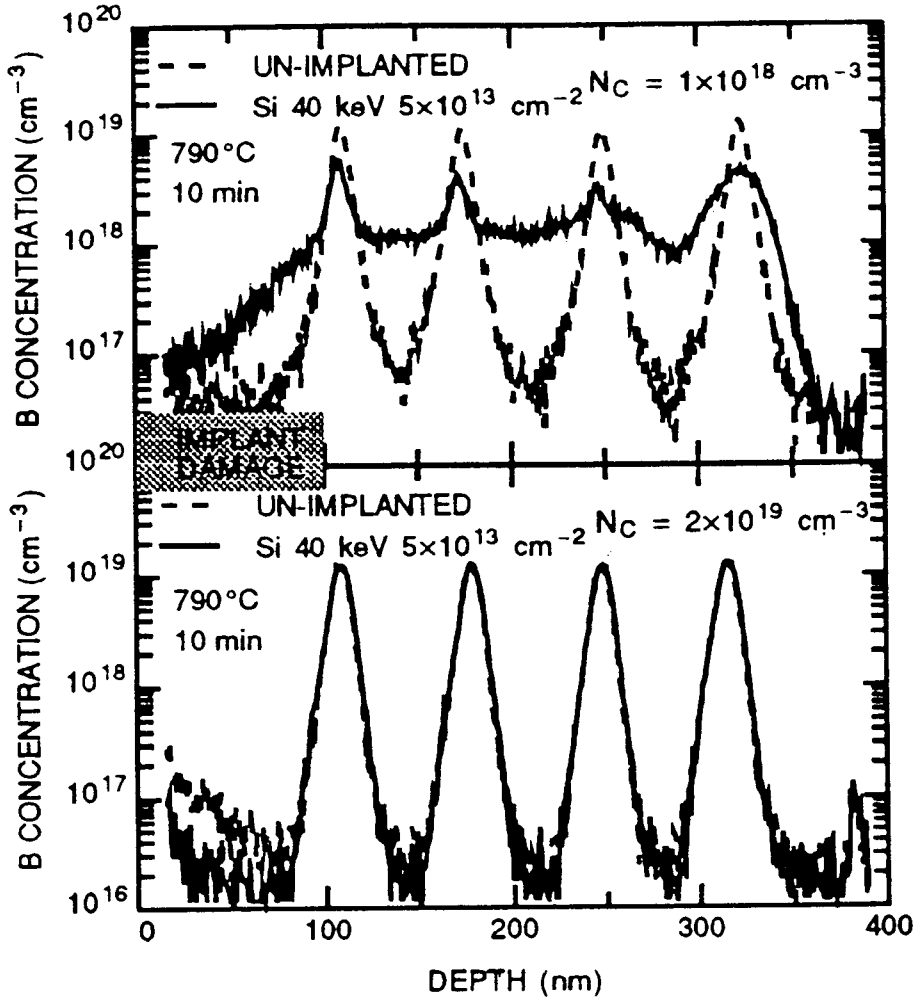

Figure 7.5: SIMS measurements showing that $2x10^{19}$ cm^{-3} background carbon concentrations suppress TED in 10^{19} cm^{-3} boron doped superlattices. [108]

7.6 Effect of Carbon on Thermal Diffusion of Boron

Following the extrinsic base implantation work, the effects of carbon on thermal diffusion (no implantation) of boron in SiGe were investigated. Previous work has shown that boron has a lower diffusivity in SiGe compared to Si which is due to the germanium atom and not related to strain [114]. Different pieces from both 50 Å doped $Si_{0.8}Ge_{0.2}$ and $Si_{0.795}Ge_{0.2}C_{0.005}$ bases with 50 Å spacers (a total thickness of 150 Å to avoid misfit dislocation formation) were annealed at various temperatures ranging from 750°C to 950°C. Devices were then fabricated from the annealed wafer pieces with the double mesa process of Figure 3.6 without any further ion-implantation or annealing. One would expect that, following a certain thermal anneal, the boron will diffuse outside of the SiGe spacers into the Si collector, forming a parasitic barrier which is not present in the as-grown wafers. This barrier will lower the outdiffused device's collector saturation currents from that of the as-grown saturation current and result in lower transistor Early voltages. In this way one can probe boron diffusion on a far more sensitive scale than possible by SIMS and minimize SIMS cost by doing SIMS only on wafers which show interesting electrical changes.

Figure 7.6 shows common base collector currents for both SiGe and SiGeC devices following thermal anneals at various temperatures. Following a 855°C, 15 minute anneal, the collector saturation current of the SiGe device has decreased by a factor of 25 compared with that of the as-grown device. The SiGeC device's collector current is identical to the as-grown collector current, however. Only after annealing the SiGeC wafers at 950°C for 15 minutes do the SiGeC device's saturation currents begin to deviate

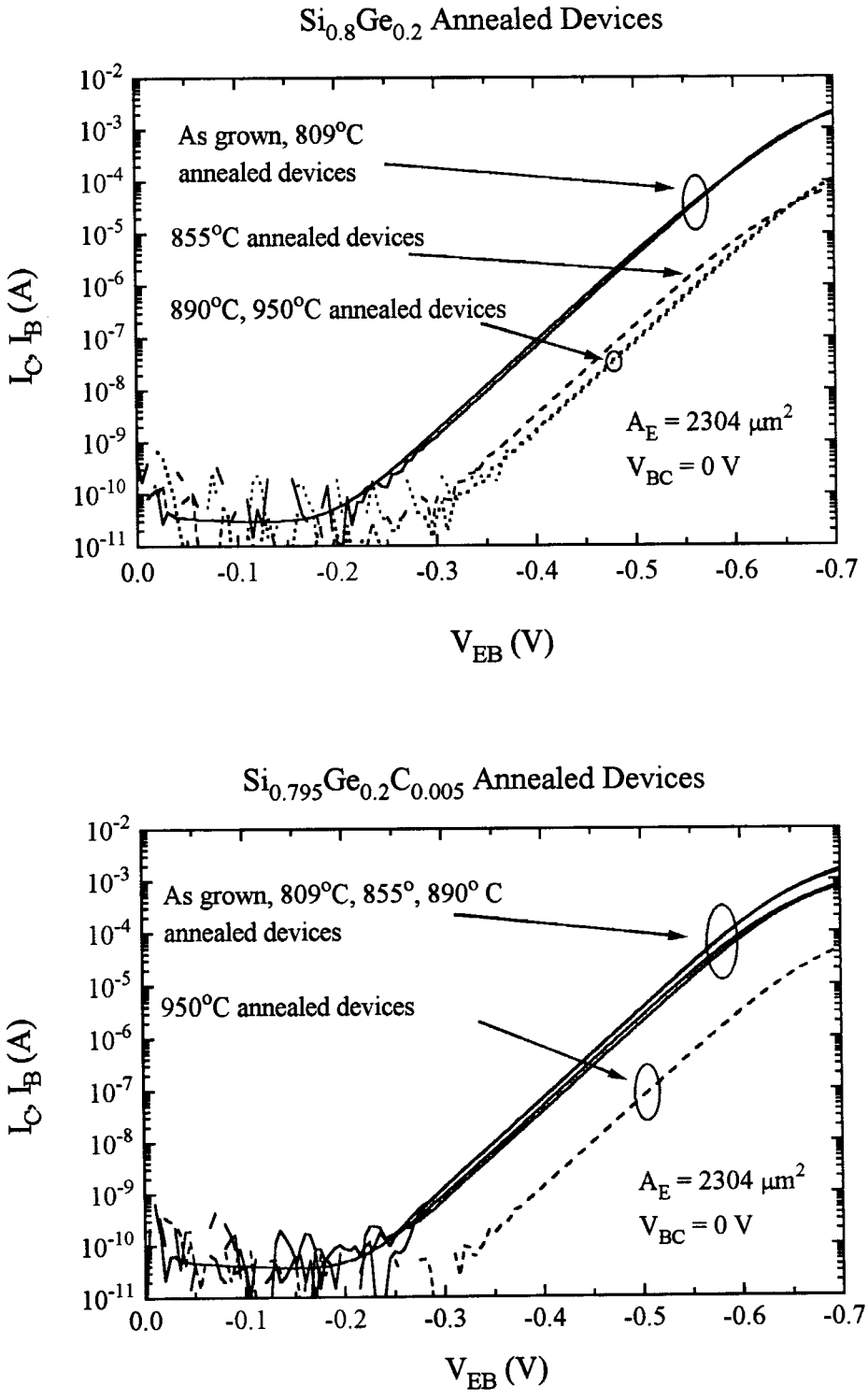

Figure 7.6: Collector currents of wafer pieces following postgrowth thermal anneal.

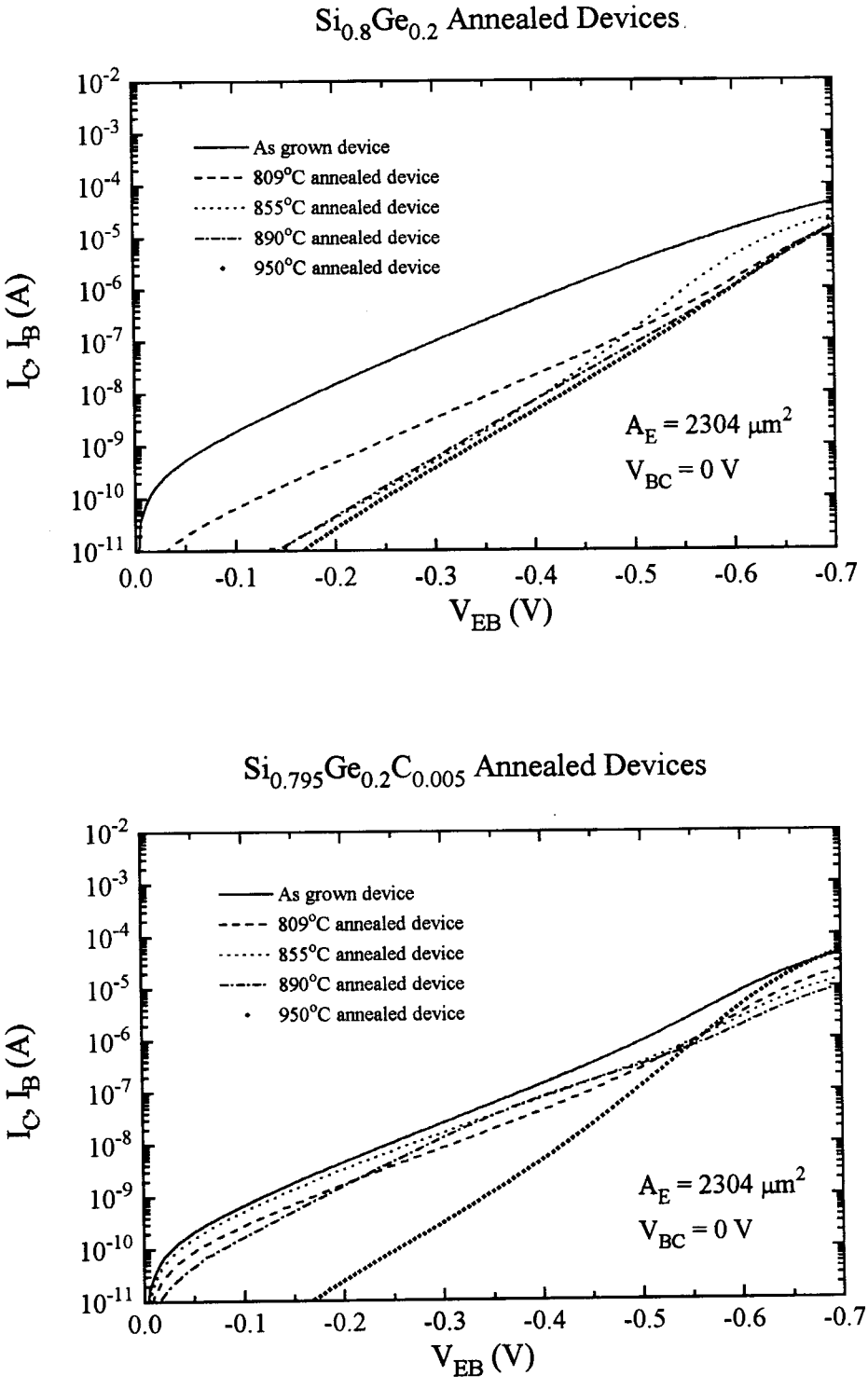

Figure 7.6b: Base currents of wafer pieces following postgrowth thermal anneal.

from the as-grown values, indicating substantial boron outdiffusion. Figure 7.7 shows common-emitter characteristics of SiGe and SiGeC annealed devices showing that the no-carbon transistor has degraded Early voltages compared with that of the carbon transistor following the 855°C anneal. These should be compared to the as-grown common-emitter characteristics which are shown in Figure 6.1. The V_A of the transistors without carbon was reduced from 50 V to 6 V by the anneal, while with carbon the V_A remained 20 V. Hence the electrical data suggests that C in SiGe reduces the thermal diffusion of boron. Pieces of the wafers annealed at 950°C which underwent defect etch showed no sign of dislocation formation, indicating that SiGe strain release is not the cause for the drop in collector saturation current. The decrease in saturation current in the $Si_{0.795}Ge_{0.2}C_{0.005}$ device following 950°C anneal may be due to boron outdiffusion, or due to new effects related to carbon defect formation at these anneal temperatures (Section 5.2). It was previously reported that the $Si_{0.795}Ge_{0.2}C_{0.005}$ device's collector saturation currents drop following a 890°C anneal. This was discovered to be in error, however. The correct temperature is 950°C.

Figure 7.8 shows SIMS of $Si_{0.8}Ge_{0.2}$ and $Si_{0.795}Ge_{0.2}C_{0.005}$ wafers following the 855°C, 15 minute anneal as well as SIMS from the as-grown 200 Å doped $Si_{0.8}Ge_{0.2}$ and $Si_{0.795}Ge_{0.2}C_{0.005}$ control bases. The annealled SIMS data and the control SIMS data come from wafers with different base widths. From the electrical characteristics in Figure 7.6, one would expect that for this temperature anneal the SiGe wafers should show evidence of boron outdiffusion in SIMS whereas the SiGeC wafers should not. The as-grown 200 Å doped control SiGe and SiGeC bases have identical peak boron concentrations and identical slopes of boron leading and trailing edges, as shown in Figure 7.8a. In the annealed devices, the SiGe device shows a slightly wider boron profile compared to that in the SiGeC device which is evidence of outdiffusion. This difficulty of

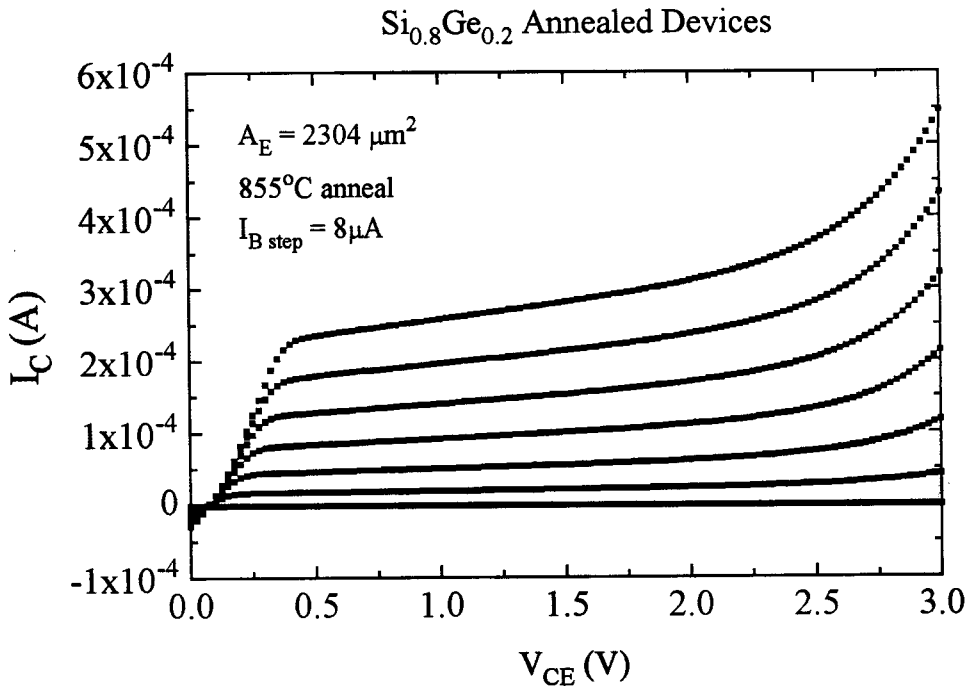

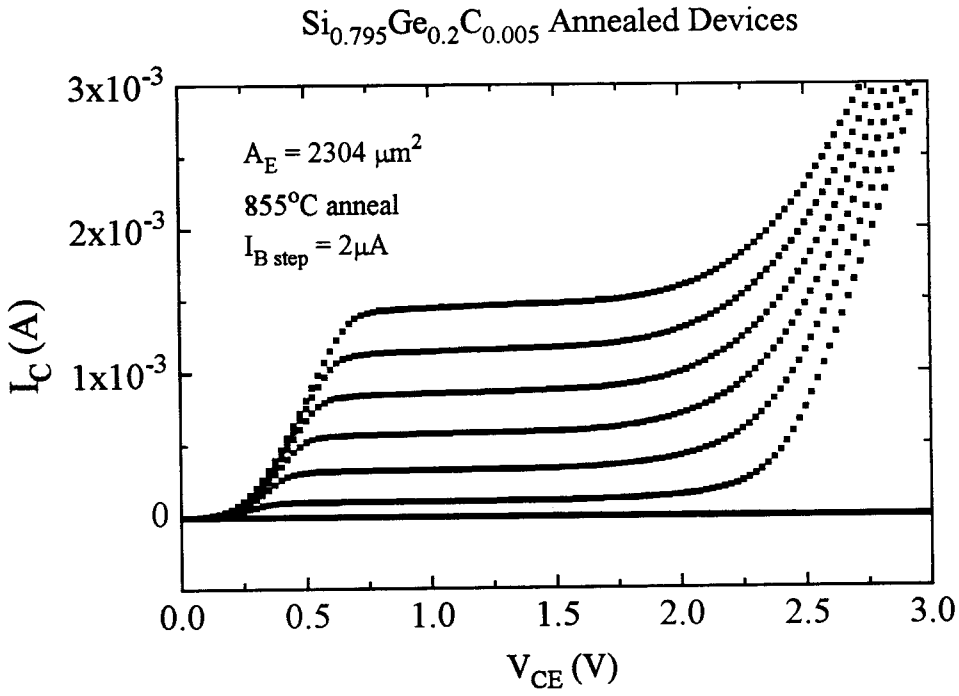

Figure 7.7: Common emitter characteristics of devices from wafer pieces following 855°C anneal.

Figure 7.8a: As-Grown Wafers

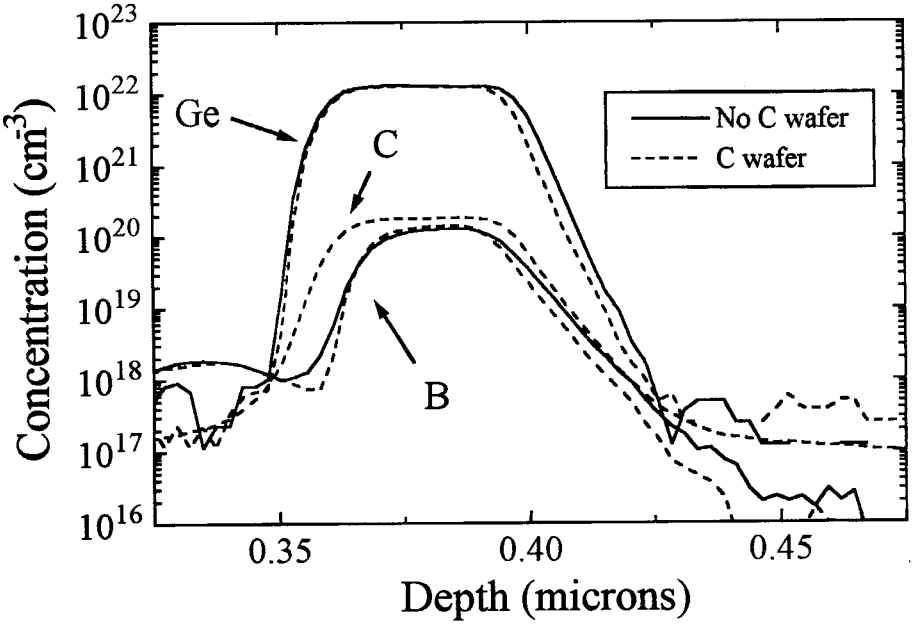

Figure 7.8b: Following 855°C, 15 min Anneal

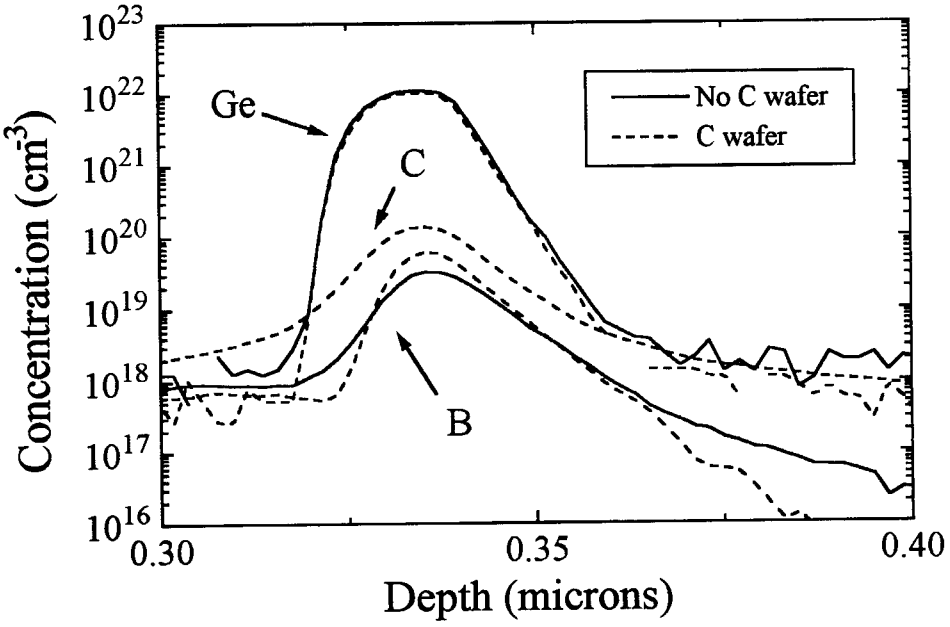

Figure 7.8: SIMS from as-grown wafers and from wafers following 855°C thermal anneal.

monitoring boron doping profiles on the order of 50 Å by SIMS alone illustrates the effectiveness of electrical means in probing boron diffusion.

7.7 Effect of Carbon on Transient Enhanced Diffusion caused by an Arsenic Emitter Implant and Anneal

While this data shows that C in SiGe can reduce the thermal diffusion of boron, the effect of carbon on boron TED caused by an arsenic emitter implant is much more striking. Pieces from the $Si_{0.8}Ge_{0.2}$ and $Si_{0.795}Ge_{0.2}C_{0.005}$ wafers underwent blanket (not masked) shallow arsenic implantation ($1.5x10^{15}$ cm^{-2} 30 keV, $3x10^{14}$ cm^{-2} 15 keV arsenic chosen to follow [109]) which used the arsenic emitter implant as the heavily doped emitter contact, as shown in Figure 7.9. Following arsenic implantation, pieces were thermally annealed at various temperatures to activate the dopants. Subsequently, double mesa transistors were fabricated as shown in Figure 7.10 without further high temperature processing. As shown previously in Figure 7.2, prior research has shown that following arsenic implantation and annealing, excess interstitials diffuse vertically to the heavily boron doped base causing the dramatically enhanced boron diffusion effects known as TED.

Figure 7.11 shows the common-base characteristics of transistors fabricated from wafers which underwent arsenic implantation and 647°C anneal along with as-grown collector currents. Note that following arsenic implantation and 647°C anneal, the collector saturation current of the SiGe devices has dropped by a factor of four and the Early voltage has been degraded to 0.5 V. This electrical data indicates that this post-growth process has caused outdiffusion of boron from the SiGe. As shown in Figure 7.11,

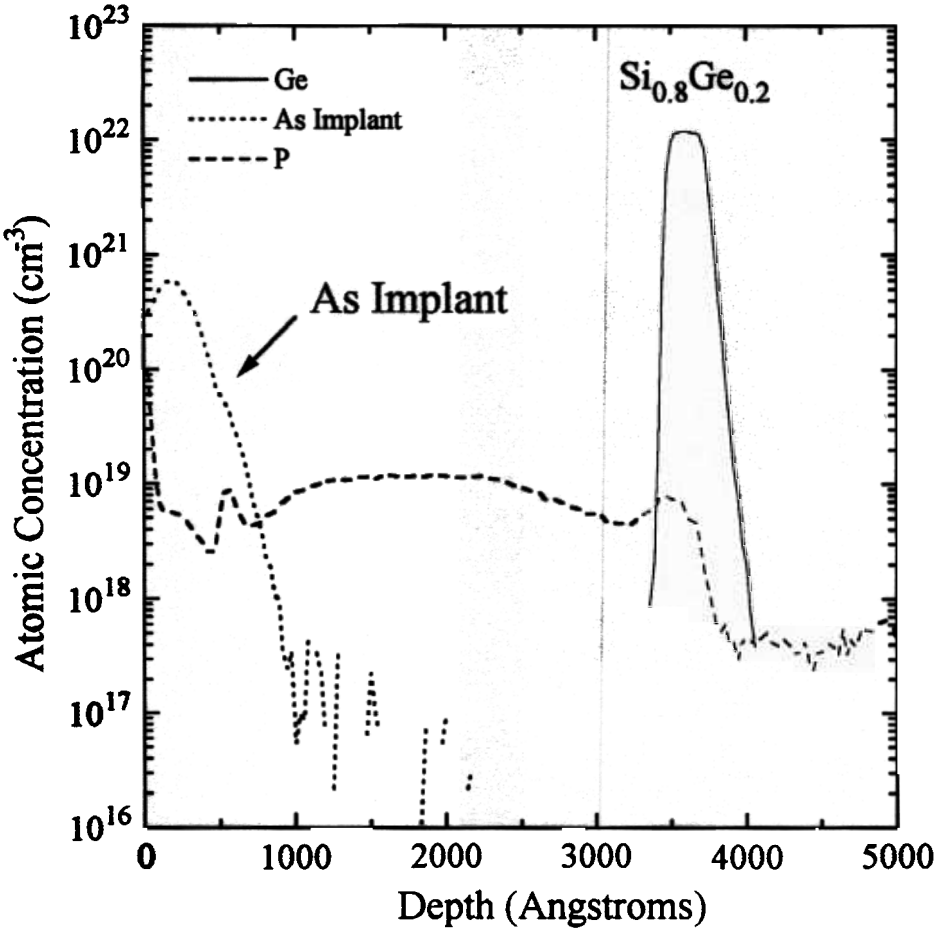

Figure 7.9: SIMS of arsenic implant following 755°C, 15 minute anneal

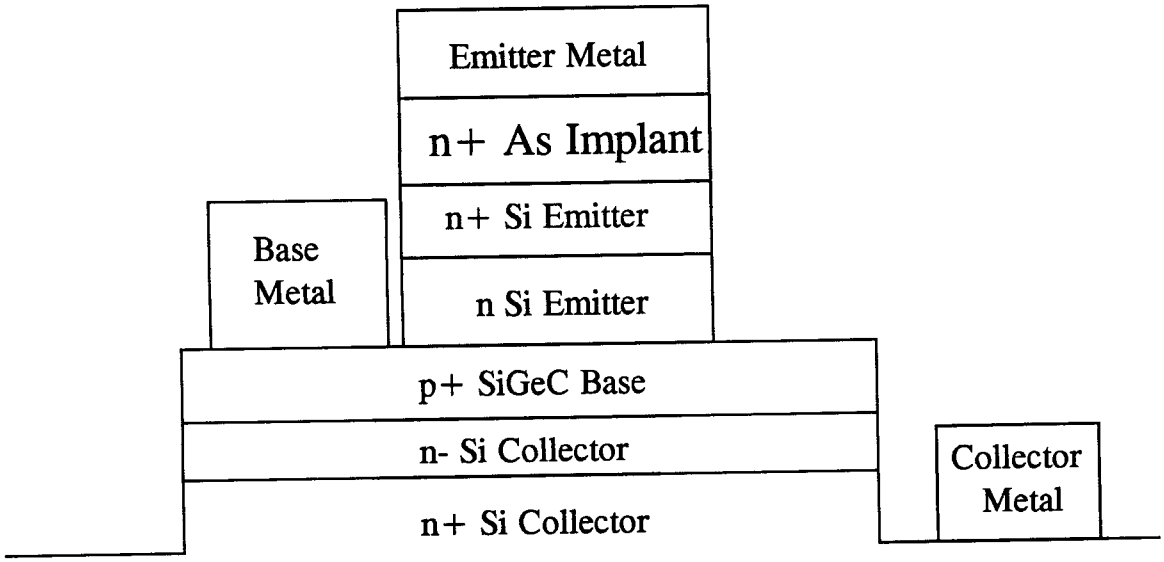

Figure 7.10: Device cross section of double mesa structure with arsenic emitter implantation.

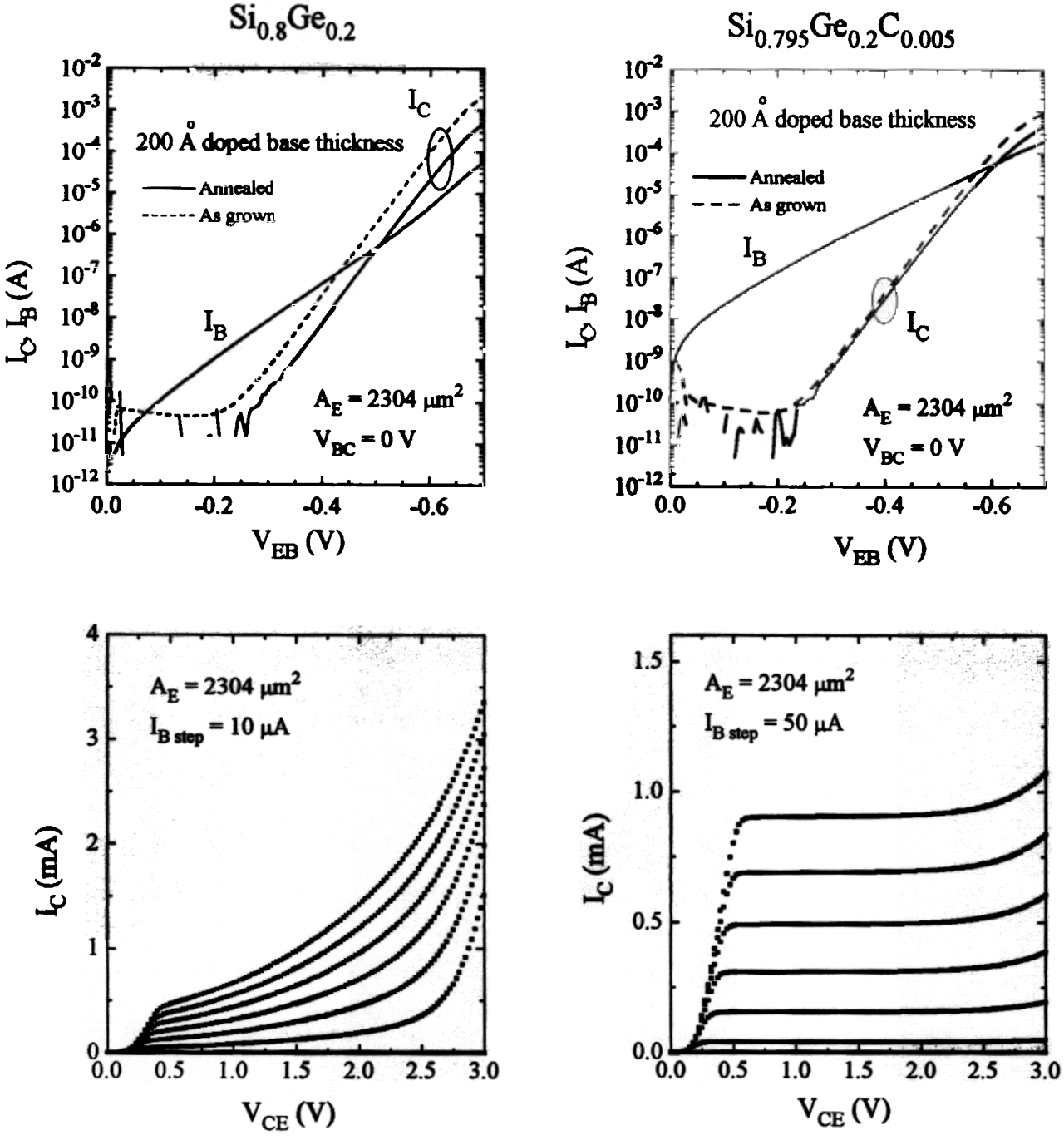

Figure 7 1: SiGe and SiGeC transistor characteristics from wafer pieces following arsenic implantation and 647°C, 15 minute anneal.

the SiGeC device's collector saturation current is identical to the as-grown collector saturation current, however, and the carbon transistor's Early voltages remain unchanged from the as-grown transistor. This data shows that the SiGe transistor has suffered the effects of TED following the 647°C anneal whereas the SiGeC devices have not. Note that the 647°C, 15 minute anneal is much less than the thermal budget the epilayers experienced during the emitter growth (700°C, 70 minutes). Since, as shown in Figure 7.6, the SiGe devices' collector currents remain unchanged following 809°C, 15 minute anneal without implantation, one may conclude that the changes in collector currents are related to TED effects.

To physically verify that carbon has indeed stopped boron TED, SIMS was performed on SiGe and SiGeC samples following arsenic implantation and 755°C anneal. As shown in Figure 7.12, the boron in the SiGe base has undergone outdiffusion, while the boron within the SiGeC base is unaltered from the as-grown profile. These profiles should be compared to Figure 7.8a showing as-grown profiles and Figure 7.8b showing profiles following 855°C anneal without ion-implantation. Hence SIMS confirms the electrical data that 0.5% carbon levels in $Si_{0.8}Ge_{0.2}$ prevents TED of 10^{20} cm^{-3} boron concentrations.

7.8 Problems in HBTs Caused by Carbon

Figure 7.13 shows Gummel Plots of SiGe and SiGeC devices fabricated from pieces which had undergone arsenic emitter implantation and 750°C, 15 minute anneal. Note that the SiGe transistor's collector saturation current has decreased by a factor of 18 from the as-grown case, which is probably due to further outdiffusion of boron compared

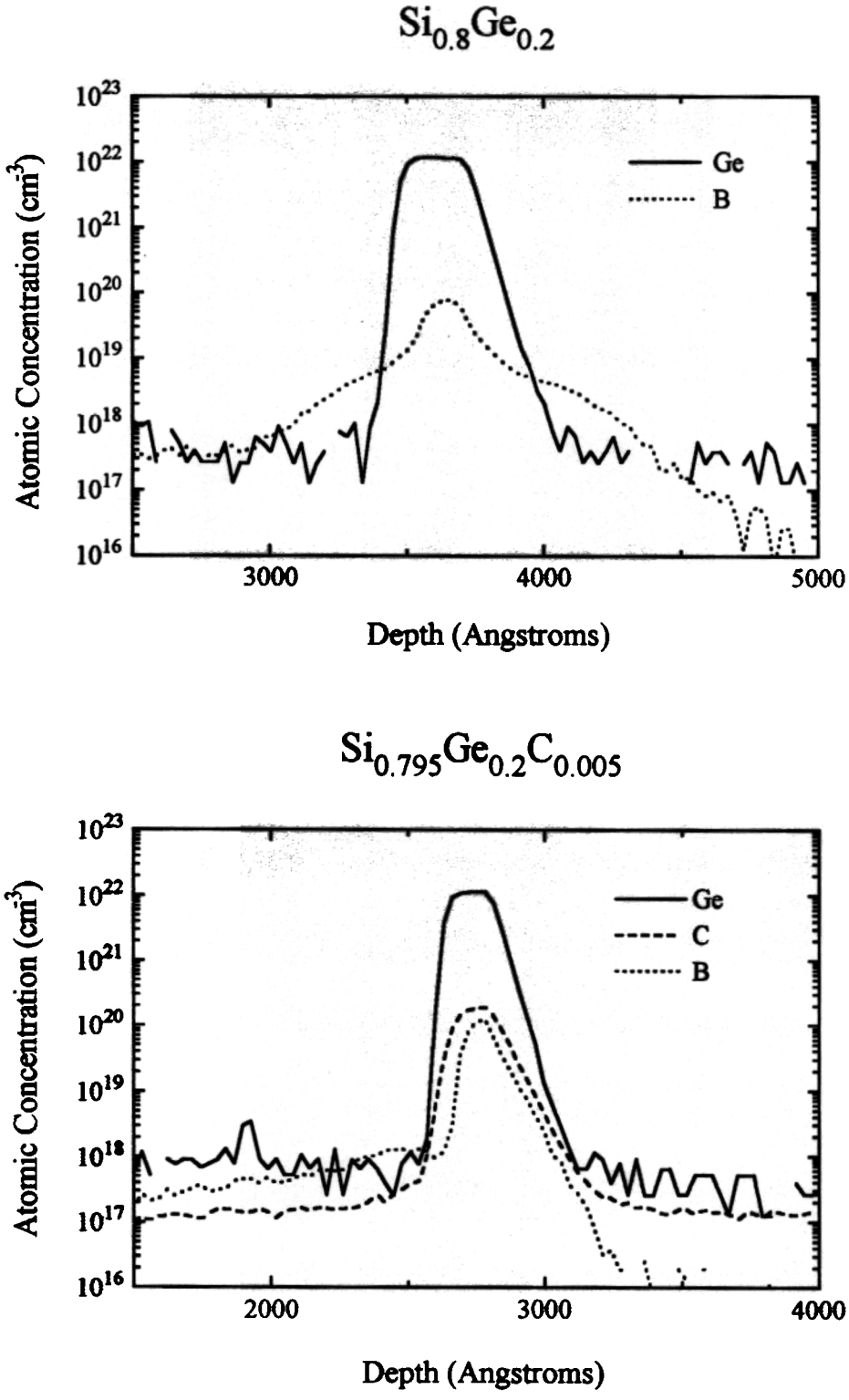

Figure 7.12: SIMS of pieces from SiGe and SiGeC wafers following arsenic implantation and 755°C, 15 minute anneal.

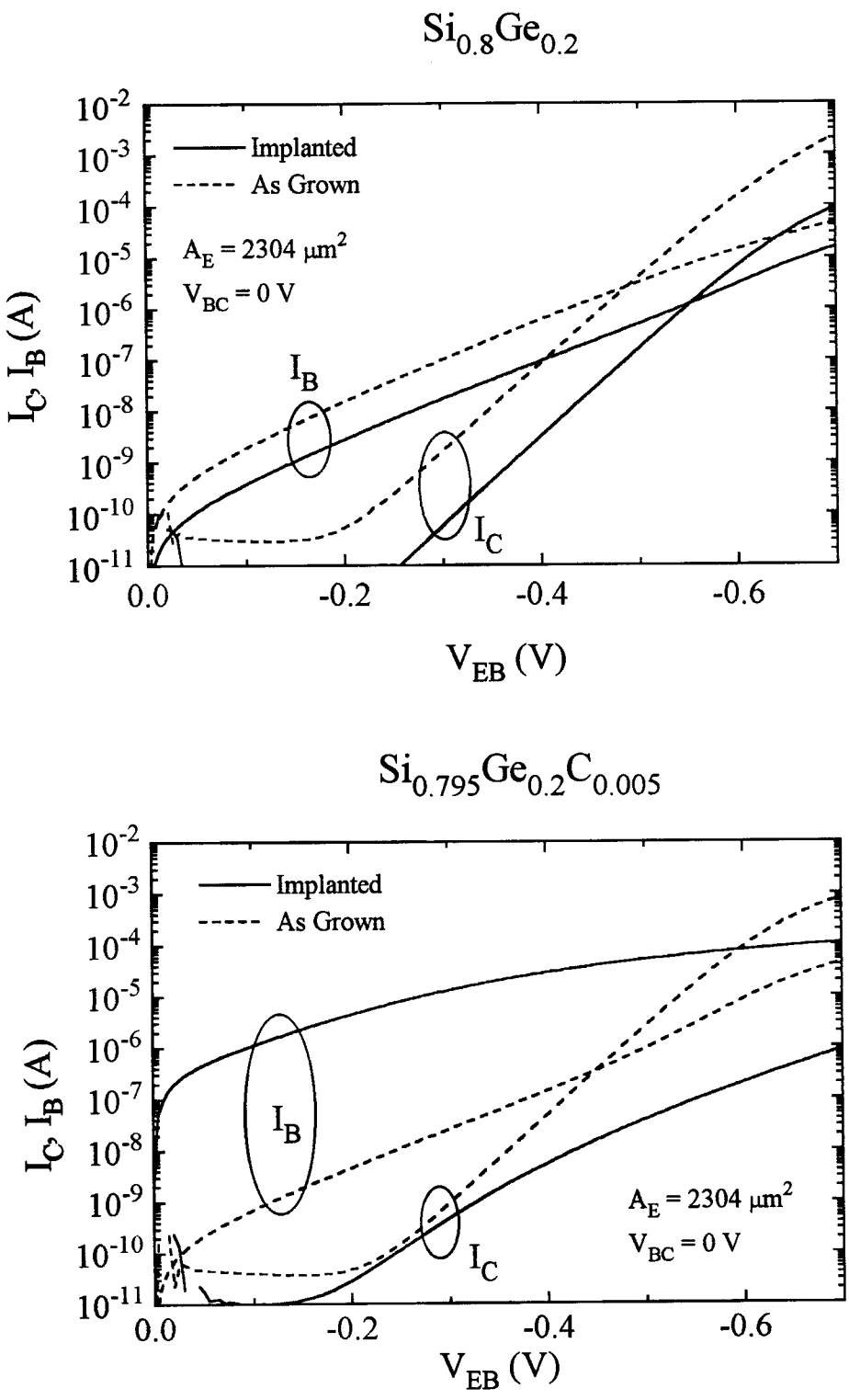

Figure 7.13: Common base characteristics of SiGe base and SiGeC base transistors fabricated from pieces following arsenic implantation and 750°C anneal.

to that following the 647°C anneal when the collector saturation current had dropped by a factor of 4. The electrical characteristics of the SiGeC devices fabricated from pieces which were arsenic implanted and annealed at 750°C bear no resemblance to the as-grown device, however. The collector current is non-ideal and is three orders of magnitude below that of as-grown transistor at high forward base-emitter bias. The base currents are orders of magnitude above the as-grown base currents. Clearly something catastrophic has occurred in the SiGeC bases during thermal anneal following arsenic implantation which does not occur in SiGe bases (Figure 7.13) or during thermal anneal of SiGeC bases without emitter implantation (Figure 7.6). Note that the collector currents of SiGeC transistors fabricated from wafer pieces not implanted but annealed at temperatures up to 950°C are still ideal and the transistors are still functioning following high temperature anneal (Figure 7.6).

Figure 7.14 shows $Si_{0.8}Ge_{0.2}$ base and $Si_{0.795}Ge_{0.2}C_{0.005}$ base I-V curves for the as-grown base-emitter diodes as well as for the base-emitter diodes following implantation and 750°C anneal. Figure 7.15 shows $Si_{0.8}Ge_{0.2}$ and $Si_{0.795}Ge_{0.2}C_{0.005}$ I-V curves for the as-grown base-collector diodes as well as for the base-collector diodes following implantation and 750°C anneal. Note that the SiGeC emitter-base diode's leakage currents are greatly enhanced following arsenic implantation and 750°C anneal. The forward bias base-collector junction characteristics of this device are unchanged following this postgrowth process, however. The diode data points the problem of SiGeC after arsenic implantation and anneal in the direction of defects created at the base-emitter junction which cause excess leakage currents. Since this effect does not occur in SiGe without carbon, carbon must be related in some way to the traps. Since it does not occur in SiGeC without implantation even with an anneal, the traps must be related in some way to implantation and anneal.

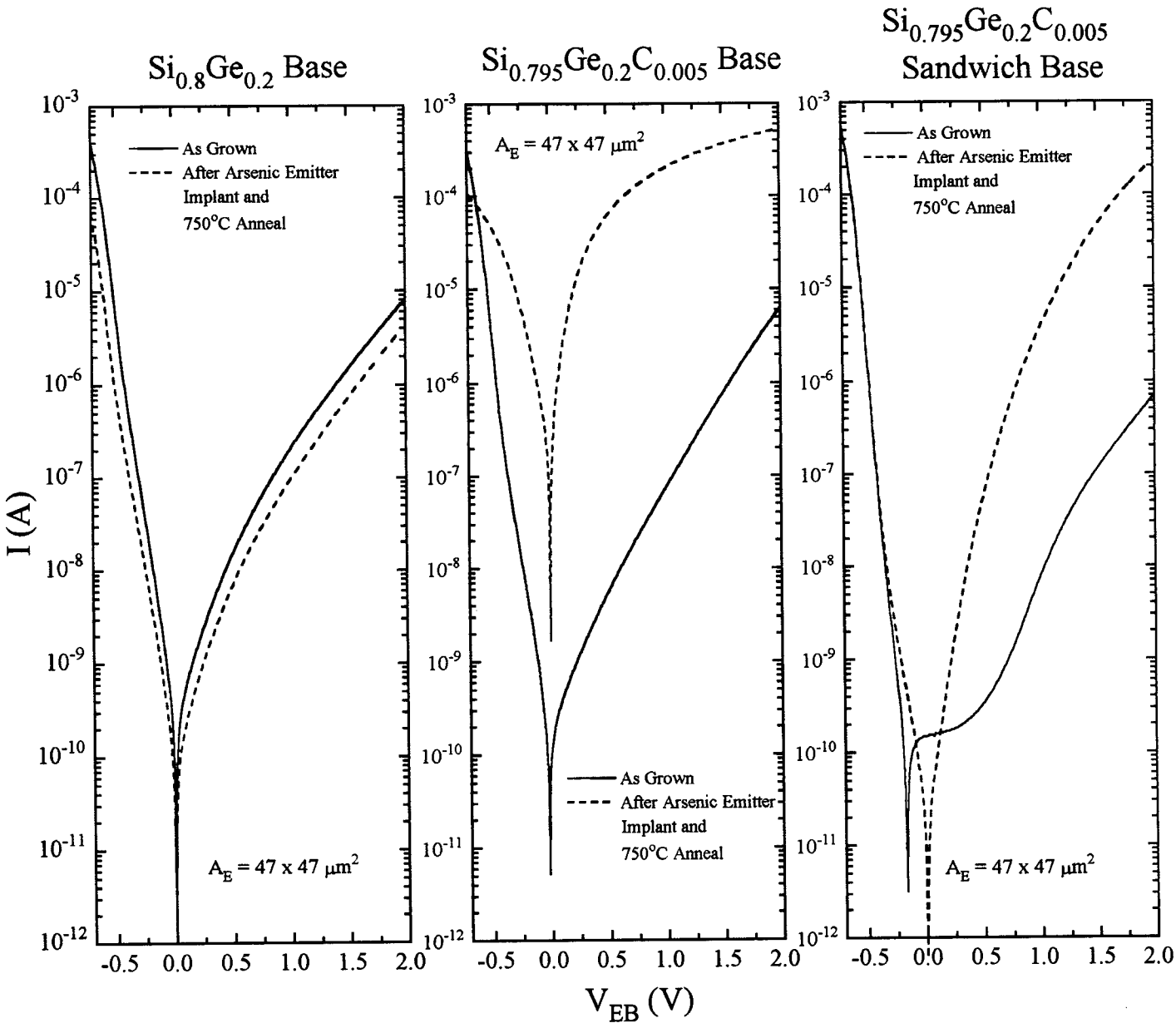

Figure 7.14: Base-emitter diode I-V curves for as-grown SiGe and SiGeC transistors and following arsenic emitter implantation and anneal. The collector was floating during the measurement.

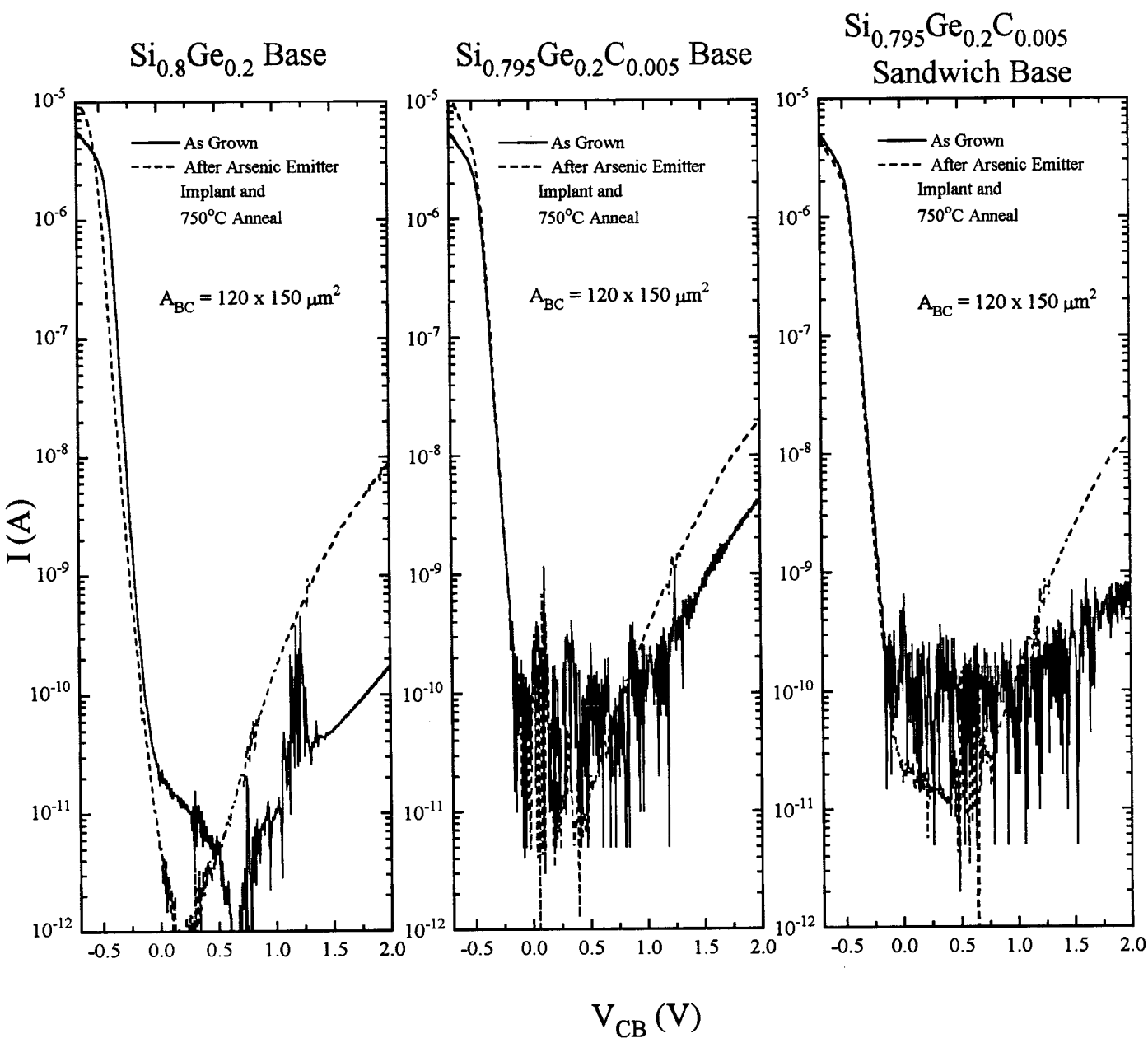

Figure 7.15: Base-collector diode curves for as-grown SiGe and for SiGeC transistors and following arsenic emitter implantation and anneal. The emitter was floating during the measurement.

The fact that carbon in silicon p-n homojunctions causes excessive leakage currents was noted previously by Poate et. al. who, in 1995, wrote that "The question still remains whether these high carbon concentrations are a practical device solution for suppressing TED as preliminary diode measurements with Si containing 10^{19} C cm^{-3} show substantial leakage and non-ideality [108]."

Considering these pieces of data alone, the outlook for C in SiGe HBTs doesn't look promising. While carbon may indeed keep boron from undergoing TED as shown in Figure 7.4 and 7.12, there is little use for it if it creates defects which kill minority carrier devices, such as diodes and bipolar devices.

7.9 Sandwich Base $Si_{1-x-y}Ge_xC_y$ HBTs

Experiments on TED caused by arsenic implantation (using the same arsenic implant as used in the previous section) were also carried out on the sandwiched base transistor wafers discussed in Chapter 6 which sandwiched 10^{20} cm^{-3} boron doped $Si_{0.8}Ge_{0.2}$ on either side of the 10^{20} cm^{-3} boron doped $Si_{0.795}Ge_{0.2}C_{0.005}$ (Figure 4.12). Undoped SiGe spacer layers also surround the doped SiGe layers, as shown in Figure 6.7. In other words, the SiGeC layer is separated from the n emitter- p base junction by the 50 Å, 10^{20} cm^{-3} boron doped SiGe spacer.

Figure 7.16 shows common-base characteristics and common-emitter characteristics for $Si_{0.795}Ge_{0.2}C_{0.005}$ sandwich base devices following arsenic implantation and anneal at 742°C for 15 minutes. The base currents in these sandwich devices are only slightly higher than those of the as-grown transistor (by a factor of 2), in contrast to characteristics of a device with a flat SiGeC base without the sandwich

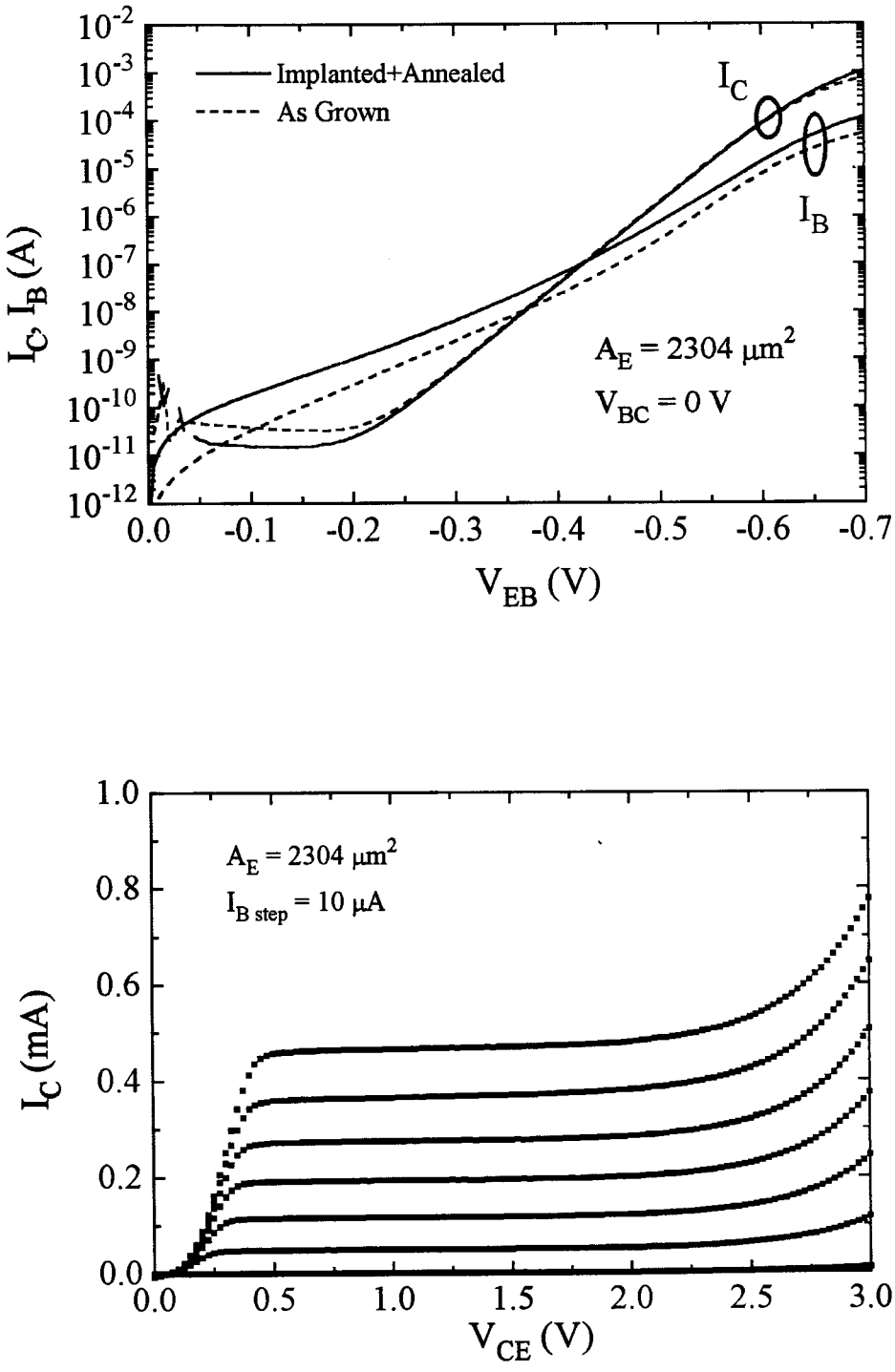

Figure 7.16: Transistor characteristic of a 0.5% C sandwich base following arsenic implantation and 742°C, 15 minute anneal.

structure shown in Figure 7.13. One may conclude that carbon in the depletion region of the emitter-base junction causes traps following arsenic implantation and annealing. Eliminating carbon from the depletion region of the device presumably puts the traps in the neutral base where they cannot cause excessive recombination currents in the base emitter depletion region. The increase in base current in the implanted and annealed device may suggest that these traps in the neutral base cause neutral base recombination. However, more experimental data is needed to determine the origin of this increase in base current.

While burying the carbon inside the doped base has apparently solved the emitter-base leakage current problem, one must also consider the effects of boron TED in the sandwich base structure. One might believe that since the boron-doped SiGe on either side of the doped SiGeC layer does not contain carbon, the boron in the doped SiGe layer should undergo TED as a result of the arsenic implantation and anneal since carbon does not exist everywhere the boron is. This would result in boron diffusion into the emitter and collector and degraded electrical characteristics. However, Figure 7.16 shows that the collector saturation current of the sandwich base device is identical to the as-grown device's saturation current. Furthermore, Figure 7.16 shows that the Early voltages of the sandwich base devices are still high following arsenic implantation and anneal. This is in direct contrast to the SiGe transistor without C anywhere which has undergone outdiffusion following arsenic implantation and 750^{o}C anneal as was shown both electrically (Figure 7.13) and by SIMS (Figure 7.12). Hence the electrical results for sandwich bases suggest that carbon has the ability to reduce boron TED effects in areas outside the carbon layer.

To verify this surprising suggestion, SIMS was performed on sandwich bases to confirm these electrical results. Figure 7.17 shows SIMS of both as-grown

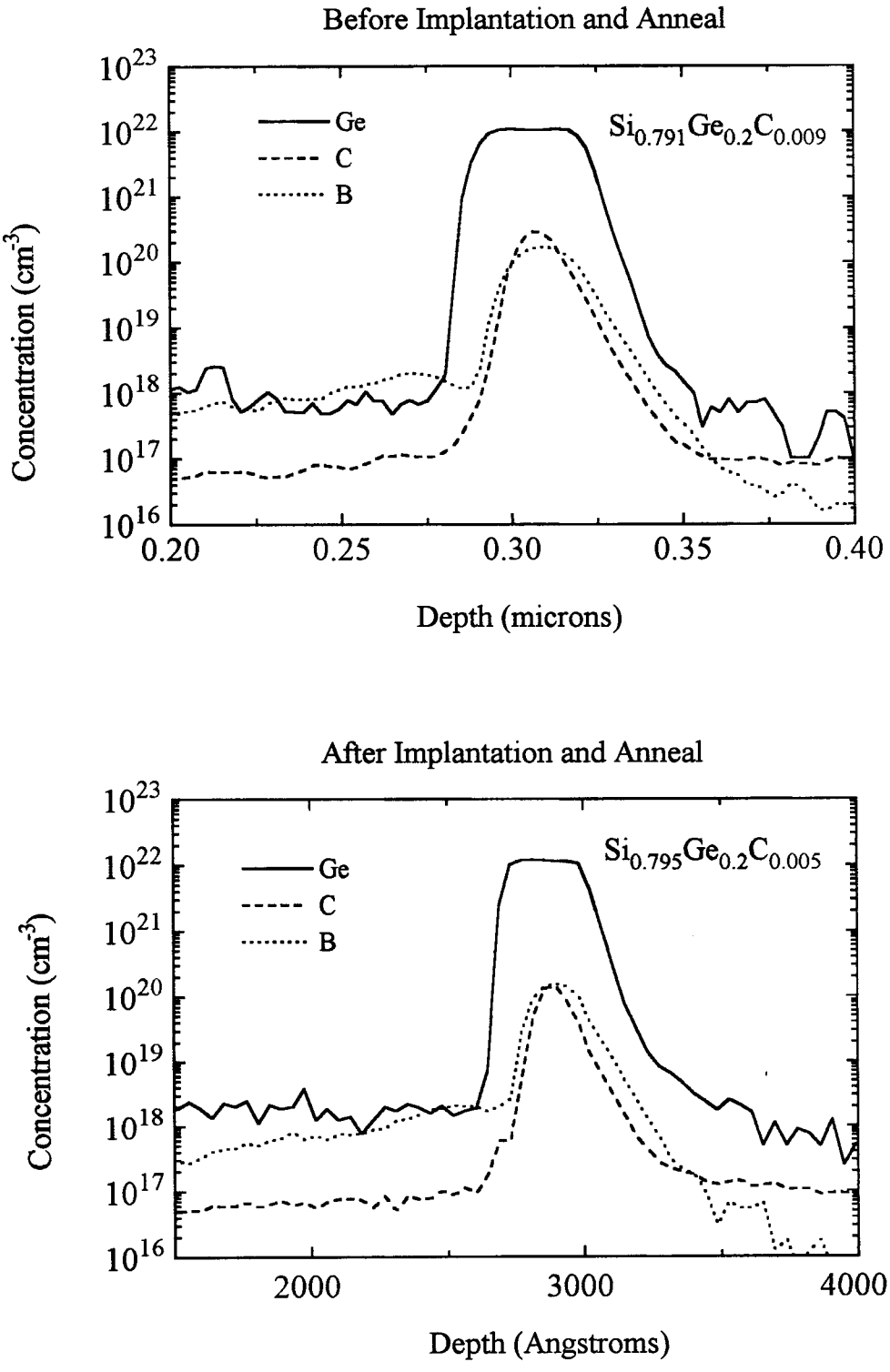

Figure 7.17: SIMS from an as-grown sandwich base and from a sandwich base following arsenic implantation and 755°C anneal.

$Si_{0.791}Ge_{0.2}C_{0.009}$ sandwich bases and $Si_{0.795}Ge_{0.2}C_{0.005}$ sandwich bases following arsenic implantation and 755°C, 15 minute anneal. In the as-grown profile, the boron layer is clearly shown to be outside the carbon profile. This is in contrast with the standard SiGeC HBT as shown in Figure 5.2, which clearly shows the boron inside both the germanium and carbon profiles, since in that device the undoped spacers do contain carbon.

Following arsenic implantation and anneal, the sandwich base boron profile is clearly unchanged from the as-grown profile, as would be expected from the electrical data of Figure 7.16. The boron outside of the carbon layers has not formed outdiffused "wings" in silicon as might be expected from Figure 7.12, a sample without carbon which has undergone similar annealing. The SIMS of Figure 7.17, along with electrical data of Figure 7.16, provided the first evidence that carbon has a non-local ability to reduce TED of boron [116]. In other words, a carbon atom in one area of a device has the remarkable ability of being able to influence boron diffusion in another area. That the boron and carbon atoms do not necessarily have to be together is quite surprising. An explanation of this nonlocal ability of C to reduce boron TED has been proposed in discussion with Conor Rafferty of Bell Labs, Lucent Technologies and is presented in the next section.

7.9 Qualitative Explanation of Experimental Data

Boron TED in Si occurs because excess interstitials generated by the implantation damage diffuse through the base during the activation anneal drastically enhancing boron diffusion [105]. During the activation anneal, this interstitial flux diffuses through the SiGe base, as shown in Figure 7.18, causing the TED effects demonstrated in Figure 7.12.

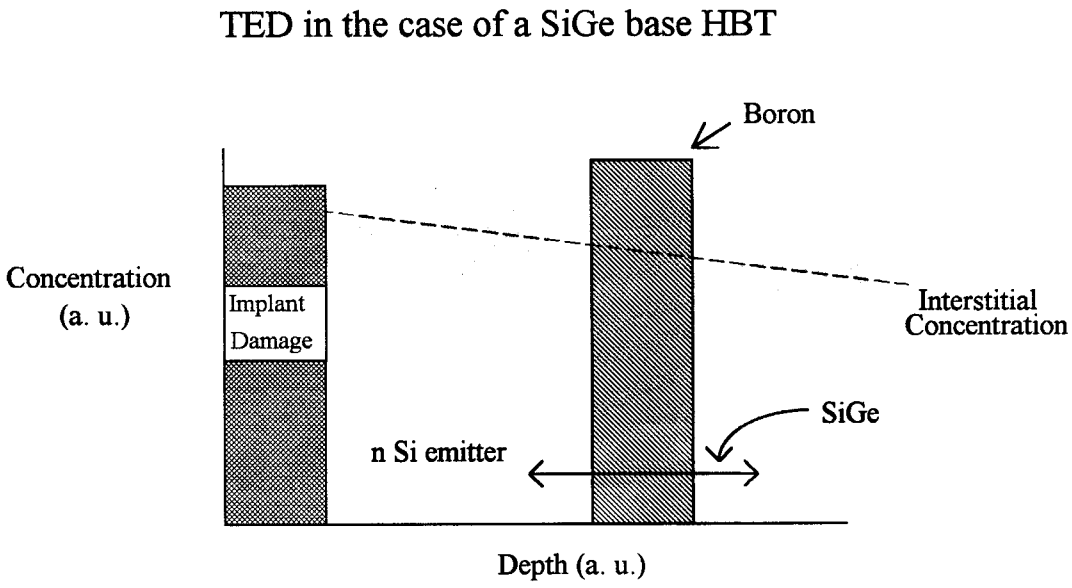

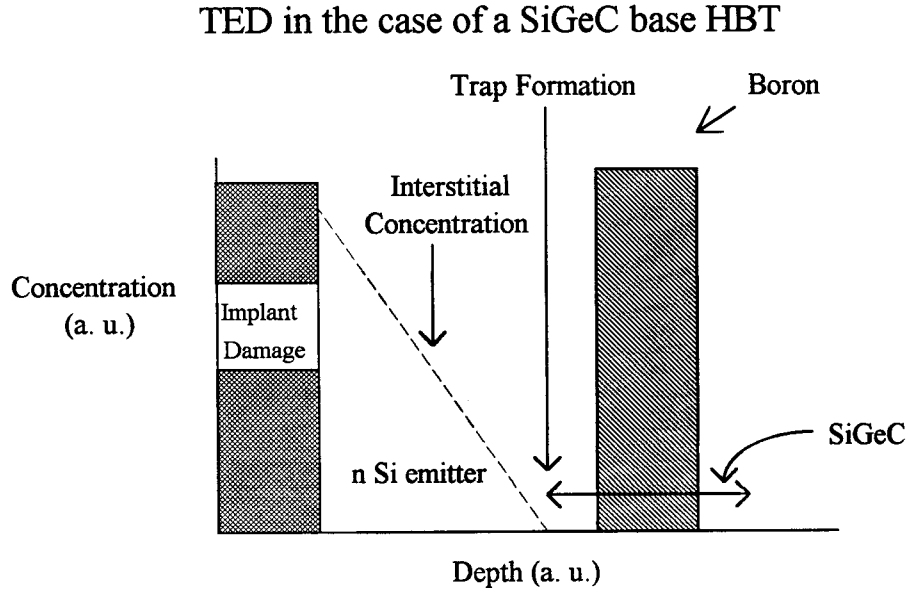

Figure 7.18: Interstitial concentration during activation anneal following arsenic emitter implant for SiGe and SiGeC HBTs.

In the case of SiGeC, however, the carbon atom acts like a silicon interstitial trap to reduce the concentration of interstitials to zero at the layer which contains carbon. Carbon in silicon has previously been known to tie up silicon interstitial atoms by creating a stable SiC complex [57]. We propose that TED does not occur in the SiGeC boron doped base because the carbon atoms similarly tie up the silicon interstitials, preventing them from causing TED of the boron buried inside the SiGeC base. Thus the boron atoms within the base never get to see the excess silicon interstitials created by the implant because they have been tied up in the undoped SiGeC spacer layer between the base and the emitter. However, the carbon atoms that trap Si interstitials in the spacer layers also lead to the diode leakage currents shown in Figure 7.14.

A schematic diagram of the interstitial concentration in the case of a standard SiGeC base transistor is shown in Figure 7.18. The interstitial concentration as a function of depth is that of the solution to the problem of a source of interstitials, the diffusion of these interstitials, and a buried sink for interstitials. The interstitial profile solution is a straight line from source to sink. This problem is analogous to the problem of the minority carrier electron distribution in the base of an actively biased bipolar transistor [95], a problem familiar to any device physicist. The source of electrons is the forward biased emitter-base junction. These electrons diffuse across the base. There is a sink at the base-collector side of the base because of the reverse-biased base collector junction.

The solution for the case of the sandwich base SiGeC HBT with boron doped SiGe outside the carbon layer is shown in Figure 7.19a and is the most interesting scenario because this device structure provides good electrical characteristics and no TED. In this case, the carbon sink inside the doped base reduces the level of interstitials to such a low amount in the SiGe boron doped layer surrounding the SiGeC layer that this small quantity of interstitials does not significantly increase the diffusion of boron in this layer! In other

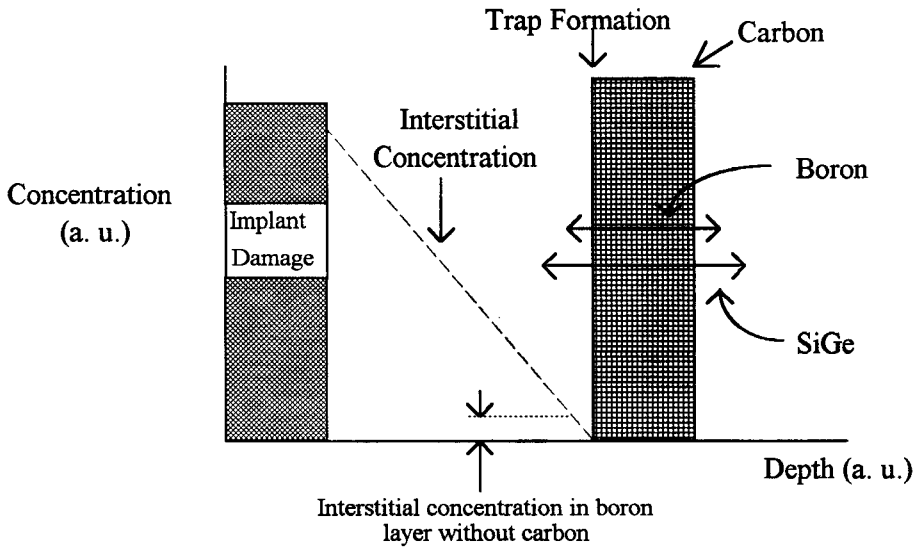

Fig. 7.19a: TED in the case of a sandwich SiGeC base HBT.

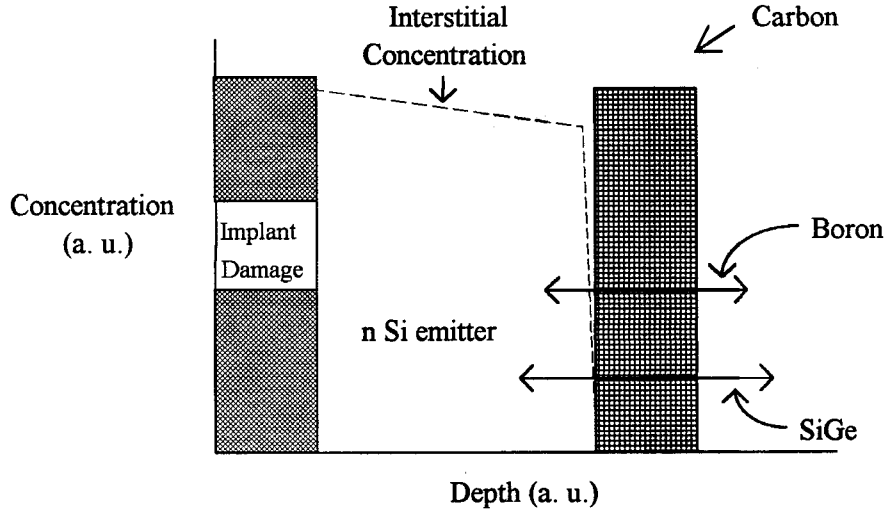

Fig. 7.19b: Incorrect solution for TED in a sandwich SiGeC HBT

Figure 7.19: Interstitial concentration during activation anneal following arsenic emitter implant for SiGeC sandwich base HBTs.

words the carbon denudes the SiGe boron doped spacer layer of the interstitials required to drive boron TED in this layer.

Note that there are other proposed solutions to the sandwich base TED problem [117]. One might ask, "Why is the solution for the profile of interstitials not a step function such as that shown in Figure 7.19b?" where the concentration of interstitials remains roughly constant until abruptly going to zero at the carbon atoms. The solution as shown in Figure 7.19a implies that interstitials at the implantation source somehow know in advance that there is a buried sink. But how should these interstitials know that there is a sink before they hit it? The Figure 7.19b solution implies no such knowledge of a sink deep in the SiGeC base. If the solution of Figure 7.19b is correct, the boron outside of the SiGeC layer in the case of the sandwich base should experience TED because the concentration of interstitials in that layer is still quite high. But, as demonstrated in Figures 7.16 and 7.17, TED does not occur.

Thus the question asked is "How do the interstitials know there is a buried sink before they actually get to it [117]?" The answer to this question is that interstitial movement, as well as that of an electron moving through the base of a bipolar transistor, is inherently diffusive, so that the interstitials undergoes a random walk before being accidentally trapped by a carbon atom. The solution featured in Figure 7.19b is incorrect for the carbon base because it is a drift solution, whereas Figure 7.19a, the correct solution, is a diffusive solution.

One remaining question to be answered is the mechanism by which the carbon atoms act as a sink for silicon interstitials. A mechanism has been proposed [57, 118] which suggests that extra atomic volume left over by the small substitutional carbon atom is an ideal spot to store a silicon interstitial, as shown in Figure 7.20. Among the many questions yet to answered are; how many interstitials can one substitutional carbon atom

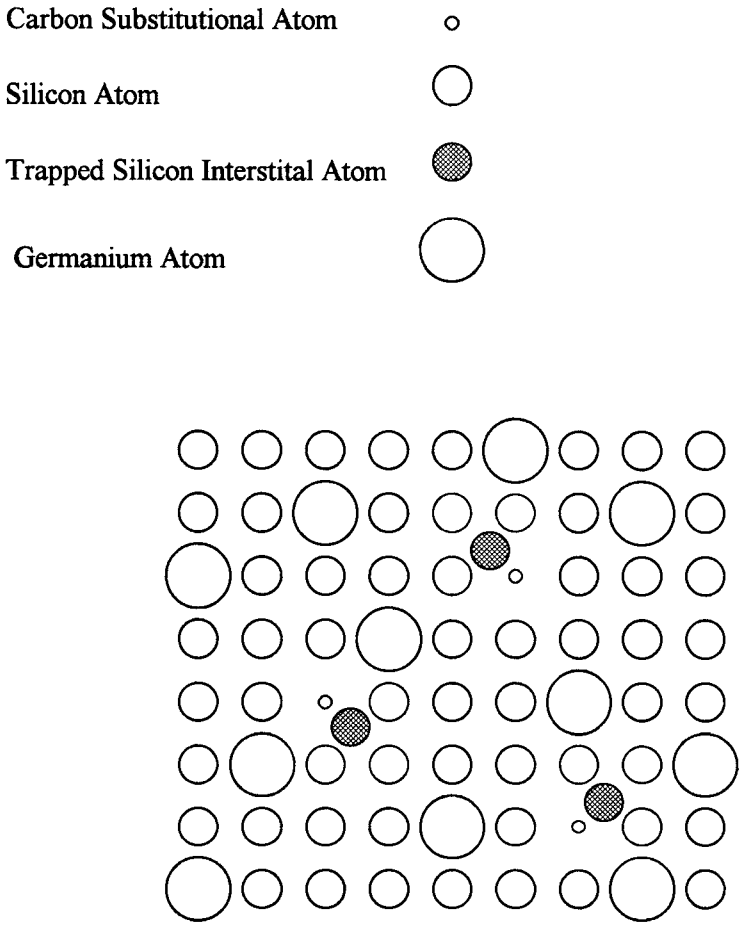

Figure 7.20: Schematic diagram illustrating the possible mechanism through which carbon atoms trap silicon interstitial atoms [117].

tie up; how are these Si-C complexes ordered; and how can one actually observe this trapping phenomenon?

If carbon atoms actually trap silicon interstitials, however, one might expect that defects form in the SiGeC layers which would be detectable by TEM. However, cross section TEM images, as shown in Figure 7.21, of SiGeC bases following arsenic implantation and high temperature anneal taken by Eric Stach at University of Virginia clearly show that the SiGeC layer following implantation and high temperature anneal does not contain any detectable defects or precipitates down to a scale of 20 Å. This also shows that SiC precipitates are not the sink for interstitials and suggests a point defect process like that described above. In any case, these Si-C complexes in the emitter-base junction are probably at the root of the standard SiGeC base HBT problems (Figure 7.13) and the emitter-base leakage current problems (Figure 7.14), following arsenic emitter implantation and anneal. Note that it is known that Si-interstitial/substitutional carbon complexes give rise to deep levels in silicon [119-121]

7.11 A Final Note

The author's only concern regarding the present results and understanding is the presence of the oxygen spike at the emitter-base interface due to the gas switch between silane and DCS. Oxygen adds yet another degree of freedom to carbon and interstitial interactions and it has been noted that carbon and oxygen can interact to form new type of defects [57]. These experiments should be in principle redone with transistors grown with DCS emitters to verify that carbon in the depletion region and not a silicon interstitial-oxygen-carbon complex is responsible for the device behavior shown in Figure 7.13.

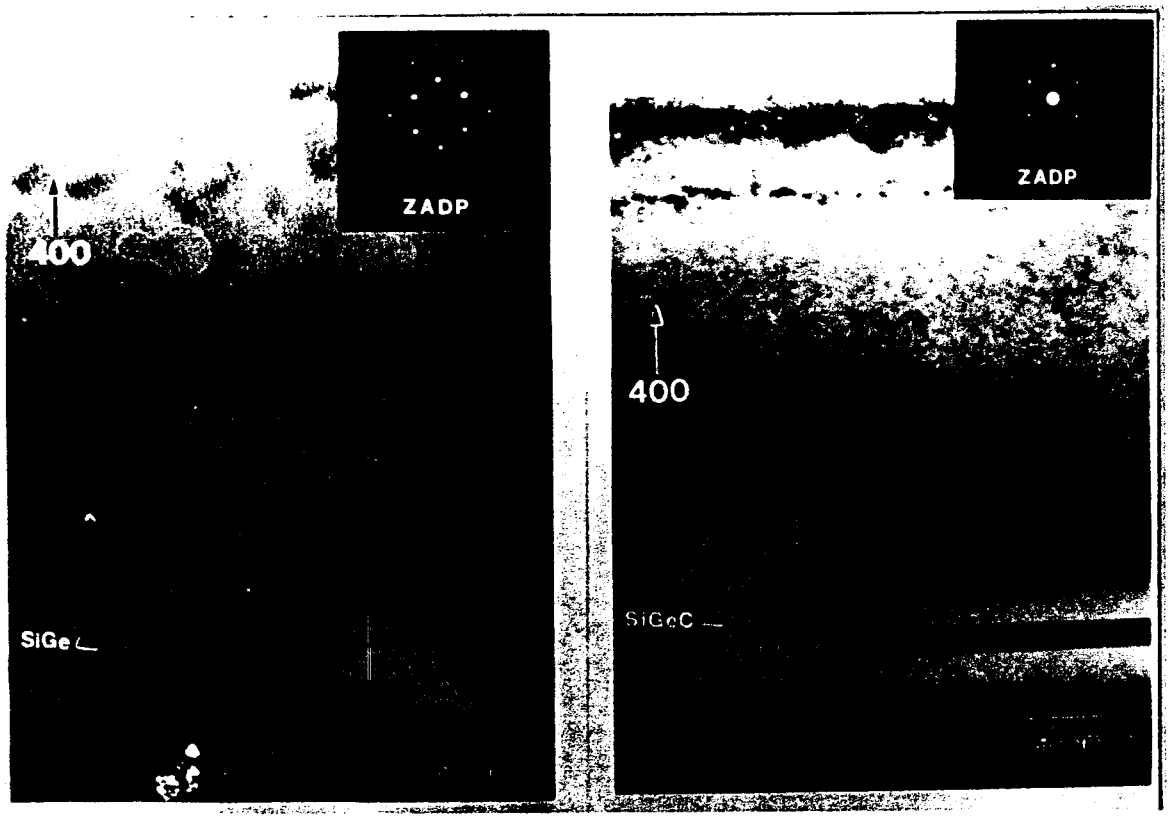

Figure 7.21: TEM micrograph of SiGe and SiGeC base HBT layers following Arsenic implantation and high temperature annealing.

However, one should keep in mind that both the SiGeC as well as the SiGe control samples contained this oxygen spike at the emitter-base interface.

It is important to note that other mechanisms besides carbon have been shown to mitigate the effects of TED conditions on boron diffusion. Ghani et. al. have shown that 10^{20} cm^{-3} oxygen levels in the base also prevent TED of boron [109]. The oxygen concentration in this thesis's SiGe and SiGeC bases is $2x10^{18}$ cm^{-3} which eliminates it as a possible explanation for the carbon related TED effects discussed in this chapter. In addition to oxygen, Xu et. al. have shown that the formation of PtSi on top of the arsenic implanted emitter region before high temperature dopant activation leads to dramatically reduced boron TED [122].

7.12 Summary

This chapter has shown that 0.5% C levels in heavily doped $Si_{0.8}Ge_{0.2}$ alloys can reduce thermal diffusion as well as transient enhanced diffusion of boron caused by an arsenic emitter implant and anneal. We have also shown that for minority carrier device applications such as diodes and HBTs, the carbon must be separated from the depletion regions by a doped SiGe spacer layer. Carbon suppresses the diffusion of boron by acting as an interstitial sink to reduce the concentration of interstitials in the region surrounding the carbon atoms. In this way, carbon has a non-local ability to reduce boron diffusion.

Using these discoveries, Lanzerotti fabricated SiGeC alloy HBTs with 10^{20} cm^{-3} base boron levels using an arsenic-implanted single-crystalline emitter contact which do not suffer from any boron outdiffusion effects. The demonstration of this device would have been impossible without the inclusion of carbon in the neutral base.

In conclusion, in response to the question posed by Poate et. al. [108], we have shown that carbon can indeed suppress TED without necessarily contributing excess leakage currents if the carbon is situated in the p-n junction correctly. Using carbon within the doped SiGe base may allow the possibility for new SiGe device structures.

Chapter 8

Conclusion

8.1 Summary

This thesis has addressed two issues which currently limit $Si_{1-x}Ge_x$ technology. The first is the critical thickness constraint of SiGe thin films while the second is the problems of boron diffusion in SiGe HBTs

To solve the first problem, carbon was added to $Si_{1-x}Ge_x$ films to form the ternary alloy $Si_{1-x-y}Ge_xC_y$. The electrical characteristics of $Si_{1-x-y}Ge_xC_y$ HBTs were used to measure a change in bandgap of + 26 meV/%C between $Si_{1-x-y}Ge_xC_y$ and $Si_{1-x}Ge_x$ for carbon fractions less than 1% for layers commensurate on Si(100) for germanium fractions of 20%. This result is similar to bandgap measurements made by photoluminescence spectroscopy.

To address the second problem, carbon was discovered to reduce thermal diffusion and transient enhanced diffusion of boron in $Si_{1-x-y}Ge_xC_y$ films. This was shown using both the electrical properties of transistors and SIMS measurements. Carbon was also discovered to have a non-local ability to reduce boron diffusion due to the fact that substitutional carbon atoms behave as interstitial sinks. These discoveries led to the

solution of the problem of how to correctly incorporate carbon into minority carrier devices to suppress boron diffusion and to the demonstration of the first 10^{20} cm^{-3} boron doped SiGe HBTs without boron outdiffusion which used arsenic implants to form a single crystalline emitter contact.

Carbon incorporation has allowed both strain relaxation and boron diffusion reduction in $Si_{1-x}Ge_x$ alloys. These results may lead to SiGe HBT structures which are more easily integrated into mainstream silicon technology.

8.2 Directions for Future Work

The fun with $Si_{1-x-y}Ge_xC_y$ has just begun.

If the results contained in this thesis stand, carbon in $Si_{1-x}Ge_x$ is an odd material indeed. Substitutional carbon in silicon is a vacuum cleaner for silicon interstitials which also kills p-n junctions. How does one balance the good aspects of carbon with the bad in mainstream silicon technology where implantation and annealing is routine? The similarities between substitutional carbon and oxygen contamination seem almost ominous.

Some future experiments include:

1) One way to prove that carbon reduces boron thermal diffusion is by growing SiGe and SiGeC HBTs with thinner and thinner undoped spacer thicknesses. Figure 4.17 shows that towards the edge of a SiGe HBT wafer, the HBTs become outdiffused due to the smaller spacer thicknesses. However, no SiGeC HBT wafers displayed this effect! The author believes that undoped spacer thickness can be reduced in

SiGeC HBTs, perhaps even to zero thickness. This belief applies to sandwich base wafers as well.

2) Sandwich base SiGeC HBTs should be fabricated using the ideal-base current process of Figure 7.1 to measure the increase in base current with carbon fraction. These devices should be compared to identical devices fabricated with a double mesa structure. With a little thought, a researcher should be able to use the same growth wafer for both experiments, thus reducing the chance for error. These devices should also be used to examine the effects of carbon-interstitial traps on carrier concentration and mobility. Carbon may also find use in other areas of the HBT, such as the doped emitter or collector regions.

(3) The carbon fraction should be varied in sandwich base HBT wafers to determine how much carbon is actually necessary to reduce TED of boron. By knowing the amount of interstitials created by an implant, one can determine how many silicon interstitials are trapped by one carbon substitutional atom.

(4) Experiments on the diffusion of boron in SiGeC should be performed similar to the experiments of P. Kuo et. al. concerning boron diffusion in SiGe [115]. For example, a spike of boron should be embedded in thick SiGeC layers of varying carbon concentrations which are then heated up to various temperatures. SIMS should then be done on each sample to see how far the boron has moved.

(5) The grandest experiment of all is that which would relate the non-local ability of carbon in reducing boron diffusion to the formation of shallow source/drain junctions for short channel MOSFETS. This idea, originally suggested by J. C. Sturm, has been said to have already been accomplished [118] using knowledge of Princeton's discovery of the non-local ability of carbon to reduce boron diffusion. Other applications of carbon to mainstream silicon technology may be equally as interesting, however.

While it is much too early to tell whether carbon will ever become applied in industry in the manner suggested by this thesis, the preliminary results are far from negative. St. Amour concluded his thesis in 1996 with the comment that "it remains to be demonstrated that either $Si_{1-y}C_y$ or $Si_{1-x-y}Ge_xC_y$ is an enabling material which allows the realization of an otherwise unattainable, useful device [20]." Only one year later, this thesis is happy to report that, yes, in fact, carbon has been used to create such a device. It was, however, created in such a manner which never could have been predicted.

References

[1] D. W. Greve, "Growth of epitaxial germanium-silicon heterostructures by chemical vapour deposition," *Materials Science and Engineering*, vol. B18, p. 22, 1993.

[2] H. Kroemer, "Heterostructure Bipolar Transistors and Integrated Circuits," *Proceedings of the IEEE*, vol. 70, p. 13, 1982.

[3] H. Kroemer, "Heterostructure bipolar transistors: What should we build?" *J. Vac. Sci. Technol. B.*, vol. 1, p. 126, 1983.

[4] H. Kroemer, "Heterostructure Device Physics: Band Discontinuities as Device Design Parameters," *VLSI Electronics: Microstructure Sciences*, vol. 10, p. 121, 1985.

[5] S. S. Iyer, G. L. Patton, J. C. Stork, B. S. Meyerson, D. L. Harame, "Heterojunction Bipolar Transistors Using Si-Ge Alloys," *IEEE Trans. Electron Devices*, vol. 36, p. 2043, 1989.

[6] H. Presting, "Challenges for SiGe-Heterotechnology," *Mat. Res. Soc. Symp. Proc.*, vol. 379, p. 417, 1995.

[7] U. Konig, "Challenges for a Si/Ge heterodevice technology," *Microelectronic Engineering*, vol. 23, p. 3, 1994.

[8] D. L. Harame, J. H. Comfort, J. D. Cressler, E. F. Crabbe, J. Y. C. Sun, B. S. Meyerson, T. Tice, "Si/SiGe Epitaxial-Base Transistors - Part 1: Materials, Physics, and Circuits," *IEEE Trans. Electron Devices*, vol. 42, p. 455, 1995.

[9] D. L. Harame, J. H. Comfort, J. D. Cressler, E. F. Crabbe, J. Y. C. Sun, B. S. Meyerson, T. Tice, "Si/SiGe Epitaxial Base Transistors- Part II: Process Integration and Analog Applications," *IEEE Trans. Electron Devices*, vol. 42, p. 469, 1995.

[10] B. Abeles and R. W. Cohen, "Ge-Si Thermoelectric Power Generator," *Journal of Applied Physics*, vol. 35, p. 247, 1964.

[11] C. A. King, J. L. Hoyt, J. F. Gibbons, "Bandgap and Transport Properties of $Si_{1-x}Ge_x$ by Analysis of Nearly Ideal $Si/Si_{1-x}Ge_x/Si$ Heterojunction Bipolar Transistors," *IEEE Trans. Electron Devices*, vol. 36, p. 2093, 1989.

[12] T. I. Kamins, K. Nauka, R. D. Jacowitz, J. L. Hoyt, D. B. Noble, J. F. Gibbons, "Electrical and Structural Properties of Diodes Fabricated in Thick, Selectively Deposited $Si/Si_{1-x}Ge_x$ Epitaxial Layers," *IEEE Electron Device Letters*, vol. 13, p. 177, 1992.

[13] J. Matthews and A. Blakeslee, "Defects in epitaxial multilayers," *J. Crystal Growth*, vol. 27, p. 118, 1974.

[14] D. Houghton, C. Gibbings, C. Tuppen, M. Lyons, and M. Halliwell, "Equilibrium critical thickness for $Si_{1-x}Ge_x$ strained layers on (100) Si," *Appl. Phys. Lett*, vol. 56, p. 460, 1990.

[15] E. J. Prinz, *Base Transport and Vertical Profile Engineering in $Si/Si_{1-x}Ge_x/Si$ Heterojunction Bipolar Transistors*. PhD Thesis, Princeton University, 1992.

[16] Z. Matutinovic Krstelj, *Base Doping Effects and Design of Si/SiGe/Si Heterojunction Bipolar Transistors.* PhD Thesis, Princeton University, 1994.

[17] E. J. Prinz, J. C. Sturm, "Current Gain-Early Voltage Products in Heterojunction Bipolar Transistors with Nonuniform Base Bandgaps," *IEEE Electron Device Letters*, vol. 12, p. 661, 1991.

[18] J. C. Sturm, P. V. Schwartz, E. J. Prinz, and H. Manoharan, "Growth of $Si_{1-x}Ge_x$ by rapid thermal chemical vapor deposition and application to heterojunction bipolar transistors," *J. Vac. Sci. Technol. B*, vol. 9, p. 2011, 1991.

[19] J. C. Sturm, P. V. Schwartz, and P. M. Garone, "Silicon temperature measurement by infrared transmission for rapid thermal processing applications," *Appl. Phys. Lett.*, vol. 56, p. 961, 1990.

[20] A. St. Amour, *Growth and Photoluminescence of Crystalline $Si_{1-x}Ge_x$/Si and $Si_{1-x-y}Ge_xC_y$/Si Heterostructures*, PhD thesis, Princeton University, 1996.

[21] P. M. Garone, J. C. Sturm, P. V. Schwartz, S. A. Schwarz, and B. J. Wilkens, "Silicon vapor phase epitaxial growth catalysis by the presence of germane," *Appl. Phys. Lett.*, vol. 56, p. 1275, 1990.

[22] E. J. Prinz, X. Xiao, P. V. Schwartz, and J. C. Sturm, "Electrical characteristics of double-base Si/$Si_{1-x}Ge_x$/Si heterojunction bipolar transistors," *J. Vac. Sci. Technol. B*, vol. 11, p. 1193, 1993.

[23] F. Sato, T. Hashimoto, T. Tatsumi, T. Tashiro, "Sub-20 ps ECL Circuits with High-Performance Super Self-Aligned Selectively Grown SiGe Base (SSSB) Bipolar Transistor," *IEEE Trans. Electron Devices*, vol. 42, p. 483, 1995.

[24] P. Narozny, H. Dambkes, H. Kibbel, E. Kasper, "Si/SiGe Heterojunction Bipolar Transistor made by Molecular-Beam Epitaxy," *IEEE Trans. Electron Devices*, vol. 36, p. 2363, 1989.

[25] M. K. Sanganeria, K. E. Violette, M. C. Ozturk, G. Harris, D. M. Maher, "Boron Incorporation in Epitaxial Silicon using Si_2H_6 and B_2H_6 in an Ultrahigh Vacuum Rapid Thermal Chemical Vapor Deposition Reactor," *J. Electrochem. Soc.*, vol. 142, p. 285, 1995.

[26] M. Racanelli, D. W. Greve, "Insitu doping of Si and $Si_{1-x}Ge_x$ in ultrahigh vacuum chemical vapor deposition," *J. Vac. Sci. Technology B*, vol. 9, p. 2017, 1991.

[27] Z. Matutinovic-Krstelj, V. Venkataraman, E.J. Prinz, J.C. Sturm, C. W. Magee, "Base resistance and effective bandgap reduction in n-p-n Si/$Si_{1-x}Ge_x$/Si HBTs with heavy base doping," IEEE Trans. Electron Devices, vol. 43, p. 457, 1996.

[28] D. Ritter, R. A. Hamm, A. Feygenson, M. B. Panish, S. Chandrasekhar, "Diffusive base transport in narrow base InP/$Ga_{0.47}In_{0.53}As$ heterojunction bipolar transistors," *Appl. Phys. Lett.*, vol. 59, p. 3431, 1991.

[29] A. F. J. Levi, B. Jalali, R. N. Nottenburg, A. Y. Cho, "Vertical scaling in heterojunction bipolar transistors with nonequilibrium base transport," *Appl. Phys. Lett.*, vol. 60, p. 460, 1992.

[30] A. A. Grinberg and S. Luryi, "Ballistic versus diffusive base transport in the high-frequency characteristics of bipolar transistors," *Appl. Phys. Lett.*, vol. 60, p. 2770, 1992.

[31] A. A. Grinberg and S. Luryi, "Coherent Transistor," *IEEE Trans. on Electron Devices*, vol. 40, p. 1512, 1993.

[32] A. A. Grinberg and S. Luryi, "Diffusion in a short base," *Solid State Electronics*, vol. 35, p. 1299, 1992.

[33] O. Hansen, "Diffusion in a short base," *Solid State Electronics*, vol. 37, p. 1663, 1994.

[34] G. Baccarani, C. Jacoboni, and A. M. Mazzone, "Current Transport in Narrow-base transistors," *Solid State Electronics*, vol. 20, p. 5, 1977.

[35] M. Ozaydin and L. F. Eastman, "Non-equilibrium carrier transport in the base of heterojunction bipolar transistors," *Solid State Electronics*, vol. 39, p. 731, 1996.

[36] J. C. Stork and R. D. Isaac, "Tunneling in Base-Emitter Junctions," *IEEE Trans. Electron Devices*, vol. 30, p. 1527, 1983.

[37] J. A. Del Alamo and R. M. Swanson, "Forward-Bias Tunneling: A Limitation to Bipolar Device Scaling," *IEEE Electron Device Letters*, vol. 7, p. 629, 1986.

[38] Z. Matutinovic-Krstelj, E. J. Prinz, P. V. Schwartz, J. C. Sturm, "Reduction of p+-n+ Junction Tunneling Current for Base Current Improvement in Si/SiGe/Si

Heterojunction Bipolar Transistors," *IEEE Electron Device Letters*, vol. 12, p. 163, 1991.

[39] H. Jorke, H. Kibbel, K. Strohm, and E. Kasper, "Forward-Bias characteristics of Si bipolar junctions grown by molecular beam epitaxy at low temperatures," *Appl. Phys. Lett*, vol. 63, p. 2408, 1993.

[40] C. A. King, R. W. Johnson, Y. K. Chen, T. Y. Chiu, R. A. Cirelli, G. M. Chin, M. R. Frei, A. Kornblit, and G. P. Schwartz, "Integratable and Low Base Resistance Si/$Si_{1-x}Ge_x$ Heterojunction Bipolar Transistors Using Selective and Non-Selective Rapid Thermal Epitaxy," *IEDM Technical Digest*, p. 751, 1995.

[41] M. L. Yu and B. S. Meyerson, "The adsorption of PH_3 on Si(100) and its effect on the coadsorption of SiH_4," *J. Vac. Sci. Technol. A*, vol. 2, p. 446, 1984.

[42] B. S. Meyerson, "UHV/CVD Growth of Si and Si:Ge Alloys: Chemistry, Physics, and Device Applications," *Proceedings of the IEEE*, vol. 80, p. 1592, 1992.

[43] T. O. Sedgwick, P. D. Agnello, D. Nguyen Ngoc, T. S. Kuan, G. Scilla, "High phosphorus doping of epitaxial silicon at low temperature and atmospheric pressure," *Appl. Phys. Lett.*, vol. 58, p. 1896, 1991.

[44] P. D. Agnello, T. O. Sedgwick, Private Communications.

[45] A. Gruhle, Private Communications, "SiGe HBTs with very high germanium content in the base."

[46] A. Schuppen, U. Erben, A. Gruhle, H. Kibbel, H. Schumacher, and U. Konig, "Enhanced SiGe Heterojunction Bipolar Transistors with 160 GHz f_{max}," *IEDM Technical Digest*, p. 743, 1995.

[47] E. J. Prinz, P. M. Garone, P. V. Schwartz, X. Xiao, J. C. Sturm, "The Effects of Base Dopant Outdiffusion and Undoped Si1-xGex Junction Spacer Layers in Si/$Si_{1-x}Ge_x$/Si Heterojunction Bipolar Transistors," *IEEE Electron Device Letters*, vol. 12, p. 42, 1991.

[48] E. J. Prinz and J. C. Sturm, "Analytical Modeling of Current Gain-Early Voltage Products in Si/$Si_{1-x}Ge_x$/Si Heterojunction Bipolar Transistors," *IEDM Technical Digest*, p. 853, 1991.

[49] A. Pruijmboom, J. W. Slotboom, D. J. Gravesteijn, C. W. Fredriksz, A. A. van Gorkum, R. A. van de Heuvel, J. M. L. van Rooij-Mulder, G. Streutker, and G. F. A. van de Walle, "Heterojunction Bipolar Transistors with SiGe Base Grown by Molecular Beam Epitaxy," *IEEE Electron Device Letters*, vol. 12, p. 357, 1991.

[50] J. W. Slotboom, G. Streutker, A. Pruijmboom, D. J. Gravesteijn, "Parasitic Energy Barriers in SiGe HBTs," *IEEE Electron Device Letters*, vol. 12, p. 486, 1991.

[51] A. Gruhle, "The Influence of Emitter-Base Junction Design on Collector Saturation Current, Ideality Factor, Early Voltage, and Device Switching Speed of Si/SiGe HBTs," *IEEE Trans. on Electron Devices*, vol. 41, p. 198, 1994.

[52] D.A. Hodges and H. G. Jackson, *Analysis and Design of Digital Integrated Circuits*, McGraw Hill International Student Edition.

[53] J. Regolini, F. Gisbert, G. Dolino, and P. Boucaud, "Growth and characterization of strain compensated $Si_{1-x-y}Ge_xC_y$ epitaxial layers," *Materials Letters*, vol. 18, p. 57, 1993.

[54] K. Eberl, S. S. Iyer, S. Zollner, J. C. Tsang, F. K. LeGoues, "Growth and strain compensaton effects in the ternary $Si_{1-x-y}Ge_xC_y$ alloy system," *Appl. Phys. Lett.*, vol. 60, p. 3033, 1992.

[55] S. Bodnar and J. L. Regolini, "Growth of ternary alloy $Si_{1-x-y}Ge_xC_y$ by rapid thermal chemical vapor deposition," *J. Vac. Sci. Technol. A*, vol. 13, p. 2336, 1995.

[56] R. C. Newman, "Carbon in crystalline silicon," *Mat. Res. Soc. Symp. Proc.*, vol. 59, p. 403, 1986.

[57] U. Gosele, "The role of carbon and point defects in silicon," *Mat. Res. Soc. Symp. Proc.*, vol. 59, p. 419, 1986.

[58] J. A. Baker, T. N. Tucker, N. E. Moyer, R. C. Buschert, "Effect of carbon on the lattice parameter of silicon," *J. Applied Physics*, vol. 39, p. 4365, 1968.

[59] R. I. Scace and G. A. Slack, "Solubility of carbon in silicon and germanium," *Journal of Chemical Physics*, vol. 30, p. 1551, 1959.

[60] R. C. Newman and J. Wakefield, "The Diffusivity of Carbon in Silicon," *J. Phys. Chem. Solids*, vol. 19, p. 230, 1961.

[61] S. Q. Feng, J. P. Kalejs, D. G. Ast, "Carbon Precipitation in CZ and EFG Silicon," *Mat. Res. Soc. Symp. Proc.*, vol. 59, p. 439, 1986.

[62] N. Akiyama, Y. Yatsurugi, Y. Endo, Z. Imayoshi, T. Nozaki, "Lowering of breakdown voltage of semiconductor silicon due to the precipitation of impurity carbon," *Appl. Phys. Lett.*, vol. 22, p. 630, 1973.

[63] B. O. Kolbesen, A. Muhlbauer, "Carbon in Silicon: Properties and Impact on Devices," *Solid State Electronics*, vol. 25, p. 759, 1982.

[64] B. S. Meyerson, F. K. LeGoues, T. N. Nguyen, and D. L. Harame, "Nonequilibrium boron doping effects in low-temperature epitaxial silicon films," *Appl. Phys. Lett.*, vol. 50, p. 113, 1987.

[65] S. S. Iyer, K. Eberl, M. S. Goorsky, F. K. LeGoues, J. C. Tsang, and F. Cardone, "Synthesis of $Si_{1-y}C_y$ alloys by molecular beam epitaxy," *Appl. Phys. Lett.*, vol. 60, p. 356, 1992.

[66] M. S. Goorsky, S. S. Iyer, K. Eberl, F. LeGoues, J. Angilello, F. Cardone, "Thermal stability of $Si_{1-x}C_x$/Si strained layer superlattices," *Appl. Phys. Lett.*, vol. 60, p. 2758, 1992.

[67] P. O. Petterson, C. C. Ahn, T. C. McGill, E. T. Croke, and A. T. Hunter, "Characterization of $Si/Si_{1-y}C_y$ superlattices grown by surfactant assisted molecular beam epitaxy," *J. Vac. Sci. Technology B*, vol. 14, p. 3030, 1996.

[68] J. B. Posthill, R. A. Rudder, S. V. Hattangady, G. G. Fountain, and R. J. Markunas, "On the feasibility of growing dilute C_xSi_{1-x} epitaxial alloys," *Appl. Phys. Lett.*, vol. 56, p. 734, 1990.

[69] M. Todd, J. Kouvetakis, D. J. Smith "Synthesis and characterization of heteroepitaxial diamond-structured $Ge_{1-x}C_x$ (x=1.5-5%) alloys using chemical vapor deposition," *Appl. Phys. Lett.*, vol. 68, p. 2407, 1996.

[70] J. Kolodzey, P. A. O'Neil, S. Zhang, B.A. Orner, K. Roe, K. M. Unruh, C. P. Swann, M. M. Waite, S. I. Shah, "Growth of germanium-carbon alloys on silicon substrates by molecular beam epitaxy," *Appl. Phys. Lett.*, vol. 67, p. 1865, 1995.

[71] S. C. Jain, H. J. Osten, B. Dietrich, and H. Rucker, "Growth and properties of strained $Si_{1-x-y}Ge_xC_y$ layers," *Semicond. Sci. Technology*, vol. 10, p. 1289, 1995.

[72] J. Mi, P. Warren, M. Gailhanou, J. D. Ganiere, M. Dutoit, P. H. Jouneau, R. Houriet, "Epitaxial growth of $Si_{1-x-y}Ge_xC_y$ alloy layers on (100) Si by rapid thermal chemical vapor deposition using methylsilane," *J. Vac. Sci. Technol. B*, vol. 14, p. 1660, 1996.

[73] H. J. Osten, E. Bugiel, P. Zaumseil, "Growth of an inverse tetragonal distorted SiGe layer on Si (001) by adding small amounts of carbon," *Appl. Phys. Lett.*, vol. 64, p. 3440, 1994.

[74] M. Todd, P. Matsunaga, J. Kouvetakis, P. Chandrasekhar, D. J. Smith, "Growth of heteroepitaxial $Si_{1-x-y}Ge_xC_y$ alloys on silicon using novel deposition chemistry," *Appl. Phys. Lett.*, vol. 67, p. 1247, 1995.

[75] J. Kouvetakis, M. Todd, D. Chandrasekhar, and D. J. Smith, "Novel chemical routes to silicon-germanium-carbon materials," *Appl. Phys. Lett.*, vol. 65, p. 2960, 1994.

[76] J. Menendez, P. Gopalon, G. S. Spencer, N. Cave, J. W. Strane, "Raman spectroscopy study of microscopic strain in epitaxial $Si_{1-x-y}Ge_xC_y$ alloys," *Appl. Phys. Lett.*, vol. 66, p. 1160, 1995.

[77] S. Im, J. Washburn, R. Gronsky, N. W. Cheung, K. M. Yu, J. W. Ager, "Optimization of Ge/C ratio for compensation of misfit strain in solid phase epitaxial growth of SiGe layers," *Appl. Phys. Lett.*, vol. 63, p. 2682, 1993.

[78] G. He, M. D. Savellano, H. A. Atwater, "Synthesis of dislocaton free $Si_y(Sn_xC_{1-x})_{1-y}$ alloys by molecular beam deposition and solid phase epitaxy," *Appl. Phys. Lett*, vol. 65, p. 1159, 1994.

[79] R. A. Soref, "Silicon based optoelectronics," *Proceedings of the IEEE*, vol. 81, p. 1687, 1993.

[80] P. Boucaud, C. Francis, F. H. Julien, J. M. Lourtioz, D. Bouchier, S. Bodnar, B. Lambert, J. L. Regolini, "Band-edge and deep level photoluminescence of pseudomorphic $Si_{1-x-y}Ge_xC_y$ alloys," *Appl. Phys. Lett.*, vol. 64, p. 875, 1994.

[81] A. St. Amour, C. W. Liu, J. C. Sturm, Y. Lacriox, M. L. W. Thewalt, "Defect-free band-edge photoluminescence and bandgap measurement in pseudomorphic $Si_{1-x-y}Ge_xC_y$ alloy layers on Si(100)," *Appl. Phys. Lett.*, vol. 67, p. 3915, 1995.

[82] K. Brunner, W. Winter, and K Eberl, "Spatially indirect radiative recombination of carriers localized in $Si_{1-x-y}Ge_xC_y/Si_{1-y}C_y$ double quantum well structure on Si substrates," *Appl. Phys. Lett.*, vol. 69, p. 1279, 1996.

[83] P. Boucaud, J. M. Lourtioz, F. H. Julien, P. Warren, M. Dutoit, "Intersubband absorption in $Si/Si_{1-x-y}Ge_xC_y$ quantum wells," *Appl. Phys. Lett.*, vol. 69, p. 1734, 1996.

[84] A. T. Khan, P. R. Berger, F. J. Guarin, S. S. Iyer, "Band-edge photoluminescence from pseudomorphic $Si_{0.96}Sn_{0.04}$ alloy," *Appl. Phys. Lett.*, vol. 68, p. 3105, 1996.

[85] B. A. Orner, A. Khan, D. Hits, F. Chen, K. Roe, J. Pickett, X. Shao, R. G. Wilson, P. R. Berger, J. Kolodzey, "Optical Properties of $Ge_{1-y}C_y$ alloys," *J. of Electronic Materials*, vol. 25, p. 297, 1996.

[86] B. A. Orner, J. Olowalafe, K. Roe, J. Kolodzey, T. Laursen, J. W. Mayer and J. Spear, "Bandgap of Ge rich $Si_{1-x-y}Ge_xC_y$ alloys," *Appl. Phys. Lett.*, vol. 69, p. 2557, 1996.

[87] L. D. Lanzerotti, A. St. Amour, C. W. Liu, J. C. Sturm, J. K. Watanabe, N. D. Theodore, "Si/$Si_{1-x-y}Ge_xC_y$/Si Heterojunction Bipolar Transistors," *IEEE Electron Device Letters*, vol. 17, p. 334, 1996.

[88] K. Rim, S. Takagi, J. J. Welser, J. L. Hoyt, J. F. Gibbons, "Capacitance-voltage characteristics of p- Si/SiGeC mos capacitors," *Mat. Res. Soc. Symp. Proc.*, vol. 379, p. 327, 1995.

[89] F. Y. Huang, K. L. Wang, "Normal-incidence epitaxial SiGeC photodetector near 1.3 μm wavelength grown on Si substrate," *Appl. Phys. Lett.*, vol. 69, p. 2330, 1996.

[90] M. Mamor, C. Guedj, P. Baucaud, F. Meyer, D. Bouchier, S. Bodnar, J. L. Regolini, "Schottky diodes on $Si_{1-x-y}Ge_xC_y$ alloys," *Mat. Res. Soc. Symp. Proc.*, vol. 379, p. 137, 1995.

[91] F. Hebert, "N-Si_xC_{1-x}/P-Si Diode Fabricated Using Silane, 1,1,1-Trichloroethane, and Arsine at Low Tempertures," *IEEE Electron Device Letters*, vol. 12, p. 477, 1991.

[92] W. Faschinger, S. Zerlauth, G. Bauer, L. Palmetshofer, "Electrical properties of $Si_{1-x}C_x$ alloys and modulation doped Si/$Si_{1-x}C_x$/Si structures," *Appl. Phys. Lett.*, vol. 67, p. 3933, 1995.

[93] H. Kuhne and A. Fischer, "On chemical vapour deposition of $Si_{1-x-y}Ge_xB_x$ thin films with very high or very low boron contents: Parts 1 and 2," *Semicond. Sci. Technol.*, vol. 9, p. 1666, 1994.

[94] H. Holloway and S. L. McCarthy, "Determination of the lattice contraction of boron-doped silicon," *J. Appl. Phys.*, vol. 73, p. 103, 1993.

[95] B. Tillack, P. Zaumseil, G. Morgenstern, D. Kruger, G. Ritter, "Strain compensation in $Si_{1-x}Ge_x$ by heavy boron doping," *Appl. Phys. Lett.*, vol. 67, p. 1143, 1995.

[96] C. A. King, J. L. Hoyt, C. M. Gronet, J. F. Gibbons, M. P. Scott, J. Turner, "$Si/Si_{1-x}Ge_x$ Heterojunction Bipolar Transistors Produced by Limited Reaction Processing," *IEEE Electron Device Letters*, vol. 10, p. 52, 1989.

[97] J. C. Sturm, E. J. Prinz, C. W. Magee, "Graded-Base $Si/Si_{1-x}Ge_x/Si$ Heterojunction Bipolar Transistors Grown by Rapid Thermal Chemical Vapor Deposition with Near-Ideal Electrical Characteristics," *IEEE Electron Device Letters*, vol. 12, p. 303, 1991.

[98] S. M. Sze, Physics of Semiconductor Devices, p. 15, John Wiley, 1981.

[99] K. S. Jones, L. H. Zhang, V. Krishnamoorthy, M. Law, D. S. Simons, P. Chi, L. Rubin, R. G. Elliman, "Diffusion of ion implanted boron in preamorphized silicon," *Appl. Phys. Lett.*, vol. 68, p. 2672, 1996.

[100] N. E. B. Cowern, K. T. F. Janseen, H. F. F. Jos, "Transient diffusion of ion-implanted B in Si: Dose, time, and matrix dependence of atomic and electrical profiles," *J. Appl. Phys.*, vol. 68, p. 6191, 1990.

[101] D. J. Eaglesham, P. A. Stolk, H. J. Gossman, J. M. Poate, "Implantation and transient B diffusion in Si: The source of the interstitials," *Appl. Phys. Lett.*, vol. 65, p. 2305, 1994.

[102] H. S. Chao, P. B. Griffin, J. D. Plummer, C. S. Rafferty, "The dose, energy, and time dependence of silicon self-implantation induced transient enhanced diffusion at 750°C," *Appl. Phys. Lett.*, vol. 69, p. 2113, 1996.

[103] W. T. C. Fang, P. B. Griffin, J. D. Plummer, "Implant Enhanced Diffusion of Boron in Silicon Germanium," *Mat. Res. Soc. Symp. Proc.*, vol. 379, p. 379, 1995.

[104] K. S. Jones, R. G. Elliman, M. M. Petravic, P. Kringhoj, "Using doping superlattices to study transient-enhanced diffusion of boron in regrown silicon," *Appl. Phys. Lett.*, vol. 68, p. 3111, 1996.

[105] J. M. Poate, D. J. Eaglesham, G. H. Gilmer, H. J. Gossman, M. Jaraiz, C. S. Rafferty, P. A. Stolk, "Ion Implantaton and Transient Enhanced Diffusion," *IEDM Technical Digest*, p. 77, 1995.

[106] H. G. A. Huizing, C. C. G. Visser, N. E. B Cowern, P. A. Stolk, R. C. M. de Kruif, "Ultrafast interstitial injection during transient enhanced diffusion of boron in silicon," *Appl. Phys. Lett.*, vol. 69, p. 1211, 1996.

[107] H. S. Chao, P. B. Griffin, J. D. Plummer, "Influence of dislocation loops created by amorphizing implants on point defect and boron diffusion in silicon," *Appl. Phys. Lett.*, vol. 68, p. 3570, 1996.

[108] P. Schwartz, *Oxygen Incorporation During Low-Temperature Chemical Vapor Deposition and its Effects on the Electrical Properties of Epitaxial Si and* $Si_{1-x}Ge_x$ *Films*. PhD Thesis, Princeton University, 1992.

[109] T. Ghani, J. L. Hoyt, A. M. McCarthy, J. F. Gibbons, "Control of Implant-Damage-Enhanced Boron Diffusion in Epitaxially Grown n-Si/p-$Si_{1-x}Ge_x$/n-Si Heterojunction Bipolar Transistors," *J. Electronic Materials*, vol. 24, p. 999, 1995.

[110] A. Gruhle, "MBE-grown Si/SiGe HBTs with high β, f_T, and f_{max}," *IEEE Electron Device Letters*, vol. 13, p. 206, 1992.

[111] J. H. Comfort, E. F. Crabbe, J. D. Cressler, W. Lee, J. Y. C. Sun, J. Malinowski, M. D'Agostino, J. N. Burghartz, J. M. C. Stork, B. S. Meyerson, "Single Crystal Emitter Cap for Epitaxial Si and SiGe Base Transistors," *IEDM Technical Digest*, p. 857, 1991.

[112] M. J. van Dort, W. van der Wel, J. W. Slotboom, N. E. B. Cowern, M. P. G. Knuvers, H. Lifka, and P. C. Zalm, "Two-dimensional transient enhanced

diffusion and its impact on bipolar transistors," *IEDM Technical Digest*, p. 865, 1994.

[113] N. E. B. Cowern, A. Cacciato, J. S. Custer, F. W. Saris, W. vanderVorst, "Role of C and B clusters in transient diffusion of B in silicon," *Appl. Phys. Lett.*, vol. 68, p. 1150, 1996.

[114] P. A. Stolk, D. J. Eaglesham, H. J. Gossman, and J. M. Poate, "Carbon incorporation in silicon for suppressing interstitial-enhanced boron diffusion," *Appl. Phys. Lett.*, vol. 66, p. 1370, 1995.

[115] P. Kuo, J. L. Hoyt, J. F. Gibbons, J. E. Turner, D. Lefforge, "Boron diffusion in Si and $Si_{1-x}Ge_x$," *Mat. Res. Soc. Symp. Proc.*, vol. 379, p. 373, 1995.

[116] L. D. Lanzerotti, J. C. Sturm, E. Stach, R. Hull, T. Buyuklimanli, C. Magee, "Suppression of Boron Outdiffusion in SiGe HBTs by Carbon Incorporation," *IEDM Technical Digest*, p. 249, 1996.

[117] J. Mogab. Private communication.

[118] C. Rafferty. Private communication.

[119] W.J. Taylor, T.Y. Tan, U. Gosele, "Carbon Precipitation in Silicon: Why is it so difficult?" *Appl. Phys. Lett.*, vol. 62, p. 3336, 1993.

[120] G. Davies, K. T. Kun, T. Reade, "Annealing kinetics of the dicarbon radiation-damage center in crystalline silicon," *Phys. Rev. B*, vol. 44, p.12 146, 1991.

[121] C. W. Song, X. D. Zhan, B. W. Benson, G.D. Watkins, "Bistable interstitial-carbon-substitutional -carbon pair in silicon," *Phys. Rev. B*, vol. 42, p. 5765, 1990.

[122] D. X. Xu, C. J. Deters, J. P. Noel, S. J. Rolfe, N. G. Tarr, "Control of anamalous boron diffuson in the base of Si/SiGe/Si heterojunction bipolar transistors using PtSi," *Appl. Phys. Lett.*, vol. 64, p. 3270, 1994.

Appendix A

Publications and Presentations Resulting from this Thesis

Publications

1. L. D. Lanzerotti, J. C. Sturm, E. A. Stach, R. Hull, T. Buyuklimanli, and C. Magee, "Suppression of boron outdiiffusion in SiGe HBTs by carbon incorporation," to be published in Proc. Symp. Mat. Res. Soc. **469** (1997).

2. L. D. Lanzerotti, J. C. Sturm, E. Stach, R. Hull, T. Buyuklimanli, and C. Magee, "Suppression of boron transient enhanced diffusion in SiGe heterojunction bipolar transistors by carbon incorporation," *Applied Physics Letters* **79** (1997) 3125.

3. L. D. Lanzerotti, J. C. Sturm, E. Stach, R. Hull, T. Buyuklimanli, and C. Magee, "Suppression of Boron Outdiffusion in SiGe HBTs by Carbon Incorporation," *IEDM Technical Digest* (1996) 249.

4. L. D. Lanzerotti, A. St. Amour, C. W. Liu, J. C. Sturm, J. K. Watanabe, and N. D. Theodore, "Si/$Si_{1-x-y}Ge_xC_y$/Si Heterojunction Bipolar Transistors," *IEEE Electron Device Letters* **17** (1996) 334.

5. L. D. Lanzerotti, A. St. Amour, C. W. Liu, J. C. Sturm, "Si/$Si_{1-x-y}Ge_xC_y$/Si Heterojunction Bipolar Transistors," *IEDM Technical Digest* (1994) 930.

Presentations

1. L.D. Lanzerotti, J. C. Sturm, E. A. Stach, R. Hull, T. Buyuklimanli, and C. Magee, "Suppression of boron outdiffusion in SiGe HBTs by carbon incorporation," Mat. Res. Soc. Spr. Mtg., San Francisco, CA (1997).

2. L.D. Lanzerotti, J. C. Sturm, E. Stach, R. Hull, T. Buyuklimanli, and C. Magee, "Suppression of boron outdiffusion in SiGe HBTs by carbon incorporation," Int. Elec. Dev. Mtg., San Francisco (1996).

3. L. D. Lanzerotti, C. L. Chang, J. C. Sturm, T. Buyuklimanli, and C. Magee, "Electrical Bandgap Measurement of Si1-x-yGexCy using Heterojunction Bipolar Transistors," Elec. Mat. Conf., Santa Barbara, CA (1996).

4. L.D. Lanzerotti, A. St. Amour, C. W. Liu, and J. C. Sturm, "Si/$Si_{1-x-y}Ge_xC_y$/Si heterojunction bipolar transistors," Int. Elec. Dev. Mtg., San Francisco, CA (1994).

Appendix B

Growth Sequence of $Si_{0.8}Ge_{0.2}$ Base HBT

This growth sequence was used to grow Sample # 1898. The profile of this wafer is identical to that of Figure 3.3 and Figure 3.4. The collector, emitter, and base spacer layer concentrations and thicknesses are identical with the exception of a 50 Å doped base width.

Sequencer Table #0

Step #	Action	Comment
0	Control On&	Turn on Control
1	Scan On(0.3)	and Scan simultaneously
2	Set(SP7,0)&	Override power to zero
3	Set(SP4,0)&	Turn off PID Control
4	Set(SP0,0.6)	zero loop counter
5	Set(DO0,1)&	Nitrogen Off
6	SET(DO1,0)&	Hydrogen Off
7	SET(DO2,0)&	Silane Off
8	SET(DO3,0)&	Germane Off
9	SET(DO4,0)&	Diborane Off
10	SET(DO5,0)&	PH3
11	SET(DO6,1)&	X OFF
12	SET(DO7,0)&	DCS
13	SET(DO8,0)	HCL Off
14	SET(DO9,0)&	Injects Off Silane
15	SET(DO10,0)&	Germane
16	SET(DO11,0)&	Diborane
17	SET(DO12,0)&	Phosphine
18	SET(DO13,0)	DCS
19	SET(AO0,0.617)&	Toxic lines flow down
20	SET(DO15,1)	Vacuum On
21	SET(DO1,1)&	Hydrogen On
22	SET(AO1,0.212)&	(old silane->germane)
23	SET(AO2,0.168)&	(old gh4->sih4, 100 sccms 10%Si

24	SET(AO3,0.613)	Diborane HI
25	SET(AO4,0.022)	Phosphine HI
26	SET(AO5,0.01)&	Phosphine LO
27	SET(AO6,0.537)&	DCS
28	SET(AO7,0.03)	Diborane LO
29	SET(AO8,0.0)	Pump Out
30	SEQUENCER ON(0.3,1,0)	Start Sequencer #1

Sequencer Table #1

Step #	Action	Comment
0	SET(SP1,1)&	Set Layer Number
1	SET(SP2,0.0)&	Reset Loop Control
2	SEQUENCER ON(0.3,6,0)	Call Cleaning Sequence
3	WAITUNTIL(SP2>0.5)	Cleaning Sequence
4	SET(SP2,0.0)&	Reset Loop Control
5		
6	SEQUENCER ON(0.3,5,0)	Call Buffer Layer Sequencer
7	WAITUNTIL(SP2>0.5)	Buffer Layer Sequence
8		
9		
10		
11	SET(SP2,0.0)&	Reset Loop Control
12	SEQUENCER ON(0.3,4,0)	Call Silicon Layer Sequence
13	WAITUNTIL(SP2>0.5)	Silicon layer Sequence
14	SET(SP2,0.0)&	Reset Loop Control
15		
16	SEQUENCER ON(0.3,2,0)	Call Base-Emitter Sequence
17	WAITUNTIL(SP2>0.5)	Alloy Layer Sequnce
18		
19		
20	SET(SP2,0.0)&	Reset Loop Control
21		
22		
23		
24		
25		
26	SEQUENCER ON(0.3,7,0)	Call Reload Sequence
27	END	
28		
29		
30		
31		

Sequencer Table #2

Step #	Action	Comment
0	SET(DO9,1)&	inject germane
1	SET(DO13,1)&	inject dcs, ms
2	WAIT(60)	grow i sige
3	SET(DO11,1)	inject dibore
4	WAIT(60)	p SiGe
5		
6	SET(DO11,0)&	dibore off
7		
8	WAIT(60)	i SiGe
9	SET(DO9,0)&	germane inject off
10	SET(DO10,1)&	inject silane
11	SET(DO13,0)	dcs inject off
12	SET(DO2,0)	germane select off
13	SET(DO7,0)	unselect dcs
14	WAIT(15)	ge out before 700
15	SET(SP5,3.62)	700C
16	SET(DO8,0)	unselect methylsilane
17	SET(DO4,0)	unselect dibore
18	SET(DO12,1)	inject PH3
19	WAIT(780)	26 sccms emitter
20	SET(AO4,0.616)	300 sccm emitter
21	WAIT(3600)	Growing emitter
22	SET(DO10,0)&	silane off
23	SET(DO12,0)	PH3 off
24	WAIT(20)	Purge Tube
25	SET(DO3,0)	unselect silane
26	SET(DO4,0)	unselect dibore
27	SET(SP2,1.0)	
28	END	
29		
30		
31		

Sequencer Table #4

Step #	Action	Comment
0		
1		
2		
3		
4		
5		
6		
7	WAIT(30)	wait for temp at 15.5%
8	SET(SP5,3.62)	t=700
9	SET(SP4,1)	feedback on
10	WAIT(30)	wait for right temp at 700
11	SET(SP5,3.1)	t=625
12	WAIT(20)	wait for temp at 625
13	WAITUNTIL(AI24>0.5)	go for base, cut ph3 mfc
14		
15		
16		
17	SET(DO13,0)	dcs inject off
18		
19	WAITUNTIL (AI24>0.5)	open ms manual, ms up, go base
20		
21		
22		
23		
24		
25		
26		
27		
28		
29		
30	SET(SP2,1.0)&	
31	END	END

Sequencer Table #5

Step #	Action	Comment
0	WAITUNTIL(AI29<10)	Pumping Out
1	WAITUNTIL(AI24>0.5)	Open LP-Press go for buffer
2	SET(AO11,1)&	Low Pressure Select
3	WAITUNTIL(AI28<5.5)	Pressure Stabilizing
4	SET(AO8,0.60)&	Set Pressure to 6 torr
5	WAITUNTIL(AI28>5.5)	Pressure Stabilizing
6	WAIT(10)	Pressure Stabilizing
7	SET(DO13,1)&	Inject DCS
8	SET(DO12,1)&	Phosphine On
9	WAIT(300)	growing doped buffer layer
10	SET(DO12,0)	dopant off
11	WAIT(18)	undoped collector
12	SET(DO13,0)	dcs off
13	SET(AO4,0.062)	phosphine ->25 sccms
14		
15	RAMP(SP7,-0.4,0.0)	LAMPS OFF
16		
17		
18		
19		
20	WAITUNTIL(AI24>0.5)	go for cold values; cut ph3 press
21	SET(SP3,1)&	Get Cold Values
22	WAIT(1)	
23	SET(SP3,0)&	Latch Cold Values
24	RAMP(SP7,0.4,0.274)	Lamps Up to T=1000
25		
26	WAIT(60)	Clean
27	SET(DO13,1)	Inject DCS
28	WAIT(60)	Low doped collector
29	RAMP(SP7,-0.4,0.155)	ramp lamps down to 15.5%
30	SET(SP2,1.0)	
31		

Sequencer Table #6

Step #	Action	Comment
0	WAITUNTIL(AI24>0.5)	CLOSE LP-PRESS GO
1	SET(AO11,0)&	High Pressure Select
2	SET(AO8,0.250)&	Set Pressure to 250 Torr
3	SET(AO0,0.817)&	Hydrogen Flow = 4 slpm
4	WAITUNTIL (AI29>250)	Pressure Stabilizing
5		
6		
7		
8		
9		
10		
11		
12		
13		
14		
15		
16	SET(DO5,1)&	Phosphine
17	SET(DO7,1)	DCS
18	SET(DO2,1)&	select germane
19	SET(DO3,1)&	select silane
20	SET(DO4,1)&	select dibore
21	SET(DO8,1)&	select methylsilane
22	SET(DO6,1)&	set x 1
23		
24		
25		
26		
27	RAMP(SP7,0.4,0.274)	Lamps up to T=1000
28	WAIT(120)	CLEANING
29	SET(AO8,0.0)&	Pump out
30	SET(AO0,0.617)&	Set Hydrogen Flow 3 slpm
31	SET(SP2,1.0)	

Sequencer Table #7

Step #	Action	Comment
0		
1	SET(SP7,0)	lamps off
2	SET(DO12,0)&	Phosphine
3	SET(SP4,0)	Diborane
4	SET(DO10,0)&	Germane
5	SET(DO9,0)&	Silane
6	SET(DO7,0)&	Selects Off- DCS
7	SET(DO5,0)&	Phosphine
8	SET(DO4,0)&	Diborane
9	SET(DO3,0)&	Germane
10	SET(DO2,0)&	Silane
11	SET(DO1,0)	Hydrogen
12	SET(AO8,0.0)	Pump Out
13	SET(AO7,0.0)&	Flows Off-Diborane LO
14	SET(AO6,0.0)&	DCS
15	SET(AO5,0.0)&	Phosphine LO
16	SET(AO4,0.0)&	Phosphine HI
17	SET(AO3,0.0)&	Diborane HI
18	SET(AO2,0.0)&	Germane
19	SET(AO1,0.0)&	Silane
20	SET(AO0,0.0)	Hydrogen
21	WAITUNTIL (AI<0.5)	PUMP OUT
22	SET(DO15,0)	Vacuum Off
23	SET(DO8,0)	
24	SEQUENCER OFF(0)	Sequencer 0 Off
25	SEQUENCER OFF(1)	Sequencer 1 Off
26	SEQUENCER OFF(2)	Sequencer 2 Off
27	SEQUENCER OFF(3)	Sequencer 3 Off
28	SEQUENCER OFF(4)	Sequencer 4 Off
29	SEQUENCER OFF(5)	Sequencer 5 Off
30	SEQUENCER OFF(6)	Sequencer 6 Off
31	SEQUENCER OFF(7)	Sequencer 7 Off